

# Constraints on the Evolution of Black Hole Spin due to Magnetohydrodynamic Accretion

Masaaki Takahashi\*

*Department of Physics and Astronomy, Aichi University of Education, Kariya, Aichi 448-8542, Japan*

Akira Tomimatsu†

*Department of Physics, Nagoya University, Nagoya 464-8602, Japan*

(Dated: March 23, 2021)

Stationary and axisymmetric ideal magnetohydrodynamic (MHD) accretion onto a black hole is studied analytically. The accreting plasma ejected from a plasma source with low velocity must be super-fast magnetosonic before passing through the event horizon. We work out and apply a trans-fast magnetosonic solution without the detailed analysis of the regularity conditions at the magnetosonic point, by introducing the bending angle  $\beta$  of magnetic field line, which is the ratio of the toroidal and poloidal components of the magnetic field. To accrete onto a black hole, the trans-magnetosonic solution has some restrictions on  $\beta$ , which are related to the field-aligned parameters of the MHD flows. One of the restrictions gives the boundary condition at the event horizon for the inclination of a magnetic field line. We find that this inclination is related to the energy and angular momentum transport to the black hole. Then, we discuss the spin-up/down process of a rotating black hole by cold MHD inflows in a secular evolution timescale. There are two asymptotic states for the spin evolution. One is that the angular velocity of the black hole approaches to that of the magnetic field line, and the other is that the spin-up effect by the positive angular momentum influx and the spin-down effect by the energy influx (as the mass-energy influx) are canceled. We also show that the MHD inflows prevents the evolution to the maximally rotating black hole.

PACS numbers: 97.60.Lf, 95.30.Qd, 95.30.Sf

## I. INTRODUCTION

As central engines of active galactic nuclei, some compact X-ray sources and gamma-ray bursts, black hole accretion systems are generally accepted. Recently, it is also confidently expected that the magnetic field is considered to play a very important role in the black hole accretion systems [1]. In addition, Meier [2] proposed that the inner part of a black hole accretion inflow may enter a magnetically-dominated phase. Although black holes cannot support a magnetic field by themselves, they can be immersed in the magnetic field generated by currents in black hole accretion flows. Then, above an equatorial disk and between the disk and a black hole, we can expect a magnetically-dominated “magnetosphere” like our Sun or pulsars, where large-scale (global) well-ordered magnetic fields extend to distant regions, and some part of the fields extend inwardly and enter the black hole. In this magnetosphere, more magnetically important phenomena are expected.

The research of most pulsating X-ray sources as accreting neutron stars is based on the qualitative features of their spectra and their spin-up/down rates. To discuss these period changes in these sources, Ghosh & Lamb [3] studied the accretion torque on a magnetic neutron star from a Keplerian disk by solving the hydromagnetic

equations along the dipole magnetic field lines. In the black hole case, unfortunately, the spin of a black hole is unclear for every black hole candidate. This is because many uncertain factors about the black hole–accretion disk systems still remain to be understood; e.g, the black hole mass (the size of the black hole), the distribution of magnetic field and accreting plasma, and the radiative process by the accreting plasma, etc. The spin of a black hole would be of basic importance for considering the environment around the black hole and the activities of the black hole–accretion disk systems. Then, the understanding of the process of the hole’s spin change would provide an important tool for exploring the astrophysical activity of a black hole accretion system.

The evolution of black hole spin by accreting matter was first studied by Bardeen [4]. Assuming that the gas trickles down the event horizon from the inner-edge of an equatorial accretion disk, which was set to be located at the last stable circular orbit of the Kerr geometry, it was shown that a non-rotating black hole would always be span up during accretion. However, Thorne [5] showed that photon capture by a gas accreting black hole would become important in the last stages of spin-up, where photons are emitted by the accretion disk, and reported a limiting value of  $a/m \sim 0.9982$ , where  $m$  and  $a$  denote the mass and angular momentum per unit mass of the black hole, respectively. This is because the hole’s capture cross-section is greater for photons of negative angular momentum than photons of positive angular momentum. Then, the captured photons prevent complete spin-up to  $a/m = 1$ . When we consider a black hole

---

\*Electronic address: takahasi@phyas.aichi-edu.ac.jp

†Electronic address: atomi@gravity.phys.nagoya-u.ac.jp

immersed in a magnetosphere, the energy and angular momentum extraction due to a magnetic torque on the hole can be expected [6, 7]. The magnetic field also prevents the spin-up to  $a/m = 1$ .

The MHD inflow carries the total energy  $E$  and angular momentum  $L$  into a black hole. Then, the black hole will obtain mass  $\delta m = E$  and angular momentum  $\delta J = L$ , where  $J = am$ . Although in this paper we assume that the background metric does not change by the accretion process (at least within our observational timescale), the black hole will evolve in a secular timescale. That is, for example, the angular velocity, the spin and the surface area will be modified. From the hole's angular velocity  $\omega_H \equiv a/2mr_H$ , where  $r_H = m + \sqrt{m^2 - a^2}$  is the horizon's radius, we can obtain the relation

$$\delta\omega_H = \frac{1}{2mr_H\sqrt{m^2 - a^2}} \left[ L - \frac{a}{m}(m + r_H)E \right]. \quad (1)$$

We may expect that the magnetic field lines connected to the lower latitude region of the event horizon contribute to the hole's spin-up and the field lines connected to the higher latitude (polar) region of the event horizon contribute the spin-down (e.g., see [8]). To discuss the spin evolution, we need to construct a reasonable model of MHD accretion in a black hole magnetosphere.

In this paper, we consider a stationary and axisymmetric black hole magnetosphere with a magnetized accretion disk, where plasma flows stream along magnetic field lines under the ideal MHD approximation. The global magnetic fields can be generated by current in the equatorial magnetized accretion disk and its off-equatorial plasma in the disk's corona region. In this black hole magnetosphere, the magnetic field lines originated from the inner part of the accretion disk (within several gravitational radius) connect to the event horizon, and the fields from the outer part of the accretion disk extend to distant regions. The plasma ejected from the disk surface must stream inwardly toward the event horizon along the black hole-disk magnetic field lines or outwardly toward distant regions along the disk's open magnetic field lines; so that, we need both MHD "inflow" and "outflow" solutions, which are obtained from the general relativistic Bernoulli equation.

The general relativistic Bernoulli equation for magnetized flows, which is the relativistic extension from the work by Weber & Davis [9], was formulated by Camenzind [10] and Takahashi et al.[7]. We consider physically acceptable MHD accretion solutions that start from a plasma source with low velocity, which is sub-Alfvénic velocity (or sub-slow magnetosonic when we consider a hot flow). The physically acceptable accelerated inflow falls into the black hole after passing through the Alfvén point and the fast magnetosonic point. At the magnetosonic points, which are X-type (saddle type) critical points, a smooth transition from sub-magnetosonic to super-magnetosonic flows must occur. Takahashi [11] investigated the critical conditions on the trans-magnetosonic flows in the Kerr geometry, and presented the restriction

on the field-aligned flow parameters for the appearance of the magnetosonic point on the accretion solutions. In general, the task for finding a trans-magnetosonic solution is troublesome because the relations between the flow parameters are very complicated. Therefore, in this paper, we will study the trans-fast magnetosonic MHD accretion solution without the detailed analysis of the regularity conditions at the magnetosonic point, by introducing the bending angle  $\beta$  of magnetic field, which is defined as the ratio of the toroidal and poloidal components of the magnetic field. The singular term in the equation of motion of MHD plasma is incorporated in this function. We only assume that the function  $\beta$  is regular at the magnetosonic point, and then we find that the regularity condition of the trans-magnetosonic flow solution is automatically satisfied. Thus, we can easily find a trans-magnetosonic solution, when the function  $\beta(r, \theta)$  is given as a model. In former treatments about trans-magnetosonic solution (including the critical point analysis), the toroidal component of magnetic field is obtained by solving the relativistic Bernoulli equation under a *given* poloidal magnetic field. Although, in this paper, we assume a function  $\beta$  and discuss the restrictions on it by field-aligned flow parameters (see Appendix A), we can say that our approach is basically equivalent to the discussion about the toroidal magnetic field along the trans-magnetosonic flow in the former treatments.

Although we propose a new approach to solve the trans-magnetosonic solutions without the complicated regularity conditions at the magnetosonic points, the task for finding the function  $\beta = \beta(r, \theta)$  is another difficult problem, which is not discussed here. In this paper, a flux tube is considered, but the cross-section of the magnetic flux tube is not specified beforehand. Of course, we should give a consistent function  $\beta(r, \theta)$  along a magnetic field line for a black hole magnetosphere considered. To do this, we need to treat the force-balance between magnetic field lines streaming the trans-magnetosonic flows. However, by considering the relativistic Bernoulli equation, we can discuss the restrictions on the trans-magnetosonic flows in a black hole magnetosphere without a complete field configuration satisfying the force-balance equation (the relativistic Grad-Shafranov (GS) equation [12]). The GS equation would give another restrictions on flow solutions in addition to the restrictions discussed in this paper. This method for black hole accretion is the general relativistic extension from the special relativistic outgoing trans-magnetosonic flows by Tomimatsu & Takahashi [13].

In § II we review the basic equations for trans-magnetosonic flows in Kerr geometry (see also [7, 10]) and introduce the function  $\beta$ . By assuming a smooth function of  $\beta$ , we show trans-magnetosonic flows without the regularity condition analysis. In § III we solve cold trans-fast magnetosonic flow solutions. To fall into the black hole, the trans-fast magnetosonic solution must satisfy some conditions for the field-aligned flow parameters. We show these restrictions (the necessary condition) in

§ IV. Next, in § V, we present the boundary conditions at the event horizon for ingoing MHD flows. We show that the magnetic field configuration restricts the signature of energy and angular momentum fluxes across the event horizon. To specify the energy and angular momentum of MHD inflows, a model of the plasma source is necessary. But we can discuss the spin-up/down (as a secular evolution) of a rotating black hole by considering the restriction on MHD inflows at the event horizon. Finally, we give brief remarks in § VI.

## II. BASIC EQUATIONS FOR MHD FLOWS

We consider stationary and axisymmetric ideal MHD flows in Kerr geometry. The background metric is written by the Boyer-Lindquist coordinates with  $c = G = 1$ ,

$$ds^2 = \left(1 - \frac{2mr}{\Sigma}\right) dt^2 + \frac{4amr \sin^2 \theta}{\Sigma} dt d\phi - \frac{\mathcal{A} \sin^2 \theta}{\Sigma} d\phi^2 - \frac{\Sigma}{\Delta} dr^2 - \Sigma d\theta^2, \quad (2)$$

where  $\Delta \equiv r^2 - 2mr + a^2$ ,  $\Sigma \equiv r^2 + a^2 \cos^2 \theta$ ,  $\mathcal{A} \equiv (r^2 + a^2)^2 - \Delta a^2 \sin^2 \theta$ . The particle number conservation is  $(nu^\alpha)_{;\alpha} = 0$ , where  $n$  is the number density of the plasma and  $u^\alpha$  is the fluid 4-velocity. The ideal MHD condition is  $u^\beta F_{\alpha\beta} = 0$ , where  $F_{\mu\nu}$  is the electromagnetic tensor. The relativistic Polytropic relation is  $P = K\rho_0^\Gamma$ , where  $\rho_0 = nm_{\text{part}}$  is the rest mass density,  $m_{\text{part}}$  is the mass of the plasma particle and  $\Gamma$  is the adiabatic index. The equation of motion is  $T^{\alpha\beta}_{;\beta} = 0$ . The energy-momentum tensor is given by  $T^{\alpha\beta} = n\mu u^\alpha u^\beta - Pg^{\alpha\beta} + (1/4\pi)[F^\alpha_\lambda F^{\lambda\beta} + (1/4)g^{\alpha\beta} F^2]$ , where  $\mu \equiv (\rho + P)/n$  is the relativistic enthalpy and  $F^2 \equiv F^{\mu\nu} F_{\mu\nu}$ . The magnetic and electric fields seen by a distant observer are defined by  $B_\alpha \equiv (1/2)\eta_{\alpha\beta\gamma\delta} k^\beta F^{\gamma\delta}$  and  $E_\alpha \equiv F_{\alpha\beta} k^\beta$ , where  $k^\alpha = (1, 0, 0, 0)$  is the timelike Killing vector and  $\eta_{\alpha\beta\gamma\delta} \equiv (-g)^{1/2} \epsilon_{\alpha\beta\gamma\delta}$ . The poloidal component  $B_p$  of the magnetic field seen by a lab-frame observer is defined by

$$B_p^2 \equiv -B^A B_A / G_t^2 \quad (A = r, \theta) \quad (3)$$

$$= -[g^{rr}(\partial_r \Psi)^2 + g^{\theta\theta}(\partial_\theta \Psi)^2] / \rho_w^2, \quad (4)$$

where  $\Psi(r, \theta)$  is the magnetic stream function (the  $\phi$  component of the vector potential,  $A_\phi$ ). The poloidal component  $u_p$  of the velocity is defined by  $u_p^2 \equiv -u^A u_A$ . [ Here, we set  $u_p > 0$  for both ingoing flows ( $u^r < 0$ ) and outgoing flows ( $u^r > 0$ ). ]

The ideal MHD flows stream along the magnetic field lines (i.e.,  $\Psi(r, \theta) = \text{constant}$  lines), and have five field-aligned flow parameters; that is, the angular velocity of field lines  $\Omega_F(\Psi) = -F_{tA}/F_{\phi A}$ , the number flux per magnetic flux  $\eta(\Psi) = nu_p/B_p$ , the total energy  $E(\Psi) = \mu u_t - \Omega_F B_\phi / (4\pi\eta)$ , the total angular momentum  $L(\Psi) = -\mu u_\phi - B_\phi / (4\pi\eta)$  and the entropy, which is

related to  $K(\Psi)$ . The relativistic Alfvén Mach number  $M$  is defined by

$$M^2 \equiv \frac{4\pi\mu n u_p^2}{B_p^2} = \frac{\hat{\mu} u_p}{\mathcal{B}_p}, \quad (5)$$

where the term  $\mathcal{B}_p \equiv B_p / (4\pi\mu_c\eta)$  is introduced to nondimensionalize. The relativistic enthalpy can be expressed in terms of  $u_p$  and  $B_p$

$$\hat{\mu} \equiv \frac{\mu}{\mu_c} = 1 + \left(\frac{\mu_{\text{inj}}}{\mu_c}\right) \left(\frac{B_p}{u_p}\right)^{\Gamma-1} = 1 + \mu_{\text{hot}} \left(\frac{\mathcal{B}_p}{u_p}\right)^{\Gamma-1}, \quad (6)$$

where  $\mu_c = m_{\text{part}}$  and  $\mu_{\text{hot}} \equiv (\mu_{\text{inj}}/\mu_c)(4\pi\mu_c\eta)^{\Gamma-1}$ . The term  $\mu_{\text{inj}}$  is evaluated at the plasma injection point by

$$\mu_{\text{inj}} \equiv \frac{\Gamma K}{\Gamma-1} (\mu_c\eta)^{\Gamma-1} = \frac{\Gamma}{\Gamma-1} \frac{P_{\text{inj}}}{n_{\text{inj}} m_p} \left(\frac{u_p^{\text{inj}}}{B_p^{\text{inj}}}\right)^{\Gamma-1}. \quad (7)$$

The toroidal magnetic field  $B_\phi = (\Delta \sin \theta / \Sigma) F_{\theta r}$  can be expressed in terms of flow's parameters and the Alfvén Mach number, and the non-dimensional toroidal magnetic field  $\mathcal{B}_\phi$  is defined as

$$\mathcal{B}_\phi \equiv \left(\frac{1}{\rho_w}\right) \frac{B_\phi}{4\pi\mu_c\eta} = \frac{G_\phi \hat{E} + G_t \hat{L}}{\rho_w (M^2 - \alpha)}, \quad (8)$$

where  $\hat{E} \equiv E/\mu_c$ ,  $\hat{L} \equiv L/\mu_c$ ,  $\alpha \equiv g_{tt} + 2g_{t\phi}\Omega_F + g_{\phi\phi}\Omega_F^2$ ,  $G_\phi \equiv g_{t\phi} + g_{\phi\phi}\Omega_F$ , and  $G_t \equiv g_{tt} + g_{t\phi}\Omega_F$ . The locations of  $\alpha(r; \Psi) = 0$  give the inner and outer light surfaces for magnetic field lines of  $\Omega_F = \Omega_F(\Psi)$ . When  $M^2 = \alpha$  at some location, it seems that the toroidal magnetic field diverges. Such location is called the Alfvén point, because the poloidal velocity of the flow equals the Alfvén wave speed there. To realize the physical trans-Alfvénic flow, we also require the condition  $L/E = -(G_\phi/G_t)_A$  there (see [7]), where the label ‘‘A’’ indicates quantities at the Alfvén radius. When we set  $B_p > 0$  (i.e.,  $\partial_\theta \Psi > 0$ ) in the Northern hemisphere and  $B_p < 0$  in the Southern hemisphere, we obtain  $\eta > 0$  and  $\eta < 0$  in the respective hemispheres. Then, the direction of the toroidal magnetic field  $B_\phi$  is also reversed for the equatorial plane.

The poloidal equation (the relativistic Bernoulli equation) that gives the Mach number of the streaming plasma in the magnetosphere can be written as

$$\hat{e}^2 - \hat{\mu}^2 \alpha - M^4 (\alpha \mathcal{B}_p^2 + \mathcal{B}_\phi^2) = 0, \quad (9)$$

where  $\hat{e} \equiv \hat{E} - \Omega_F \hat{L}$ . The differential form of the poloidal equation (9) can be written as

$$(\ln u_p)' = \left[ \ln \left( \frac{\mathcal{B}_p}{\hat{\mu}} \right) \right]' - \frac{M^4}{H} \left[ \alpha \left( \frac{\mathcal{B}_p}{\hat{\mu}} \right)^2 + \left( \frac{\mathcal{B}_\phi}{\hat{\mu}} \right)^2 \right]' - \frac{1}{H} \alpha'. \quad (10)$$

where  $H \equiv (2/\hat{\mu}^2) (\hat{e}^2 - \hat{\mu}^2 \alpha - C_{\text{sw}}^2 \hat{e}^2)$ ,  $C_{\text{sw}} \equiv a_{\text{sw}} / (1 - a_{\text{sw}}^2)^{1/2}$  is the sound four-velocity and  $a_{\text{sw}} \equiv [(\Gamma-1)(1 - \hat{\mu}^{-1})]^{1/2}$  is the sound three-velocity. The prime is a

derivative along a stream line  $\partial_r + (B^\theta/B^r)\partial_\theta$ . It seems that the singularities at the Alfvén point and the fast and slow magnetosonic points are removed from the differential form of the poloidal equation, but we should note that the critical behavior is included in the term of  $(B_\phi^2)'$ . In fact, by substituting  $B_\phi$  expressed as equation (8) for equation (10), we obtain the traditional expression; that is,  $(\ln u_p)' = \mathcal{N}/\mathcal{D}$ , where the numerator  $\mathcal{N}$  and the denominator  $\mathcal{D} \propto (u_p - u_{\text{AW}})^2(u_p - u_{\text{FM}})(u_p - u_{\text{SM}})$  are the functions of  $M^2$ ,  $r$  and  $\Psi$  with field-aligned flow parameters (see [7] and [11] for the analysis at the magnetosonic points). The terms  $u_{\text{AW}}$ ,  $u_{\text{FM}}$ ,  $u_{\text{SM}}$  are the Alfvén wave speed, the fast and slow magnetosonic wave speeds, respectively.

When we assume a magnetic flux function  $\Psi = \Psi(r, \theta)$  and try to solve the poloidal equation, we need to specify a set of five field-aligned parameters satisfying the critical conditions at the X-type magnetosonic points and the Alfvén point. To obtain a physical trans-magnetosonic flow solution, the fine-tuning of the parameters is required. In general this task is very complicated. However, we now propose a new analytical method to study the trans-magnetosonic flows without the critical conditions. We can relate the toroidal magnetic field to the poloidal magnetic field by defining the bending angle of a magnetic field line as

$$\beta(r, \theta) \equiv \frac{B_\phi}{B_p}. \quad (11)$$

Then, in the differential form of the poloidal equation (10),  $(\beta^2)'$  takes the place of  $(B_\phi^2)'$ . When  $\beta$  is a smooth function at the magnetosonic points, which is a natural situation on accretion problems, there is no need to analyze the regularity condition there. That is, in the  $r$ - $u_p$  plane, the inclination  $(u_p)'$  of a flow solution is determined with a finite value anywhere. At the event horizon, the toroidal magnetic field becomes  $B_\phi^H = (-g_{\phi\phi}/\Sigma)_H^{1/2}(\omega_H - \Omega_F)(\partial_\theta\Psi)_H$  and  $\Psi(r_H, \theta) = \text{finite}$ , which are the boundary conditions there. The label ‘‘H’’ indicates quantities at the event horizon. Then, we find the condition  $\beta_H = (-g_{\phi\phi})_H^{1/2}(\omega_H - \Omega_F)$ . Thus, we can obtain physical accretion solutions passing through the event horizon with a finite Mach number.

We also introduce the poloidal electric-to-toroidal magnetic field amplitude ratio  $\xi^2$  seen by a zero angular momentum observer (ZAMO) as (see also [13])

$$\xi^2(r, \theta) \equiv \left(\frac{\overline{E}_p}{\overline{B}_T}\right)^2 = \frac{G_\phi^2}{\rho_w^2} \left(\frac{\overline{B}_p}{\overline{B}_T}\right)^2, \quad (12)$$

where we use the following relations  $\overline{E}_p^2 \equiv -\overline{E}^A \overline{E}_A = (G_\phi/\rho_w)^2 \overline{B}_p^2$ ,  $\overline{B}_p^2 \equiv -\overline{B}^A \overline{B}_A = \alpha_Z^2 B_p^2$ ,  $\overline{B}_T^2 \equiv -\overline{B}^\phi \overline{B}_\phi = (B_\phi/\rho_w)^2$ . The magnetic and electric fields seen by a ZAMO are defined by  $\overline{B}_\alpha \equiv (1/2)\eta_{\alpha\beta\gamma\delta} h^\beta F^{\gamma\delta}$  and  $\overline{E}_\alpha \equiv F_{\alpha\beta} h^\beta$ , where  $h^\beta = (h_Z^t, 0, 0, h_Z^\phi) = \alpha_Z^{-1}(1, 0, 0, \omega)$  is the four-velocity of a ZAMO seen by a distant observer (see

[14]). The term  $\alpha_Z \equiv 1/(g^{tt})^{1/2} = (\Sigma\Delta/A)^{1/2}$  is the lapse function and  $\omega = -g_{t\phi}/g_{\phi\phi}$  is the angular velocity of a ZAMO with respect to a distant observer. Then, we obtain the relation  $\xi^2 = -g_{\phi\phi}(\Omega_F - \omega)^2/\beta^2$ . At the event horizon, we obtain  $\xi_H^2 = 1$ . Although the definitions and formalisms introduced in this section are available for hot MHD flows ( $P \neq 0$ ), in the following section for the sake of simplicity let’s consider the cold MHD flows ( $P = 0$ ).

### III. COLD TRANS-FAST MAGNETOSONIC FLOW SOLUTIONS

For a cold MHD flow ( $\hat{\mu} = 1$ ) the poloidal equation (9) is reduced to

$$AM^4 - 2BM^2 + C = 0, \quad (13)$$

where

$$A = \left(z - \frac{1}{\beta^2}\right) \frac{1}{\rho_w^2} (G_\phi \hat{E} + G_t \hat{L})^2, \quad (14)$$

$$B = \hat{e}^2 - \alpha, \quad (15)$$

$$C = \alpha(\hat{e}^2 - \alpha) \quad (16)$$

with  $z \equiv -(k+1)\rho_w^2/(G_\phi \hat{E} + G_t \hat{L})^2$ , and  $k \equiv (g_{\phi\phi} \hat{E}^2 + 2g_{t\phi} \hat{E} \hat{L} + g_{tt} \hat{L}^2)/\rho_w^2$ . Then, the Alfvén Mach number of the flow is solved by

$$M_\pm^2(r, \theta) = \frac{B \pm (B^2 - AC)^{1/2}}{A}, \quad (17)$$

where  $M_+^2$  denotes super-Alfvénic solution ( $M^2 > \alpha$ ) and  $M_-^2$  denotes sub-Alfvénic solution ( $M^2 < \alpha$ ). The discriminant of the quadratic equation is denoted by

$$B^2 - AC = \frac{\alpha + \beta^2}{\rho_w^2 \beta^2} (G_\phi \hat{E} + G_t \hat{L})^2 (\hat{e}^2 - \alpha). \quad (18)$$

Although the locations of the Alfvén point are given by the flow parameters  $L/E$  and  $\Omega_F$  for each magnetic field line  $\Psi = \text{constant}$ , the distribution of the Alfvén surfaces in a black hole magnetosphere is obtained when the magnetic field distribution  $\Psi = \Psi(r, \theta)$  and the boundary conditions at the plasma source  $E = E(\Psi)$ ,  $L = L(\Psi)$  and  $\Omega_F = \Omega_F(\Psi)$  are specified. The plasma source (the plasma injection point) is located within the sub-Alfvénic region, where the poloidal flow velocity is less than the Alfvén wave speed, and the neighborhood of the event horizon and the distant region from the plasma source are in the super-Alfvénic region, where the poloidal flow velocity is greater than the Alfvén wave speed. The accretion/wind solution is denoted by  $M^2 = M_-^2$  in the sub-Alfvénic region and by  $M^2 = M_+^2$  in the super-Alfvénic region. Both branches of the solutions always connect smoothly at the Alfvén point, where  $B^2 - AC = 0$ ; that is,  $(M_+^2)_A = (M_-^2)_A = \alpha_A$ . Furthermore, at the light surfaces, we see that  $(M_-^2)_L = 0$ , while  $(M_+^2)_L = 2\hat{e}^2/A_L$

is finite except the case that  $A_L = 0$  accidentally. The label ‘‘L’’ indicates quantities at the light surfaces.

If the coefficient  $A$  becomes zero at some location for a given magnetic field line specified by  $\xi^2 = \xi^2(r; \Psi)$ , the Mach number  $M_+^2$  of the super-Alfvénic flow solution diverges there, while  $M_-^2$  has a finite value in the sub-Alfvénic region. This means that such a magnetic field line under a given flow’s parameter set is *unphysical* in the super-Alfvénic region. In fact, from equations (5) and (8) both the toroidal magnetic field  $\mathcal{B}_\phi$  and the poloidal magnetic field  $\mathcal{B}_p$  should vanish at the location of  $A = 0$ , where  $M^2 = M_+^2 \rightarrow \infty$ . (Note that, although  $(\mathcal{B}_\phi)_{A=0} = (\mathcal{B}_p)_{A=0} = 0$ , the ratio  $\beta$  must have a finite value of  $\beta^2 = 1/z$  at  $A = 0$ .) Thus, such a solution (where  $A = 0$  in the super-Alfvénic region) can not be accepted as a solution of trans-magnetosonic accretion/wind. To obtain a physically acceptable MHD flow, the magnetic field configuration characterized by such a function  $\xi = \xi(r, \theta)$  should be modified to avoid the appearance of  $A = 0$  location, or another set of flow parameters should be selected at the plasma source.

For the inflow (or outflow) streaming toward the black hole (or distant regions), if  $A = 0$  on the sub-Alfvénic flow, the solution has a finite Mach number across this location. However, if  $A = 0$  in the super-Alfvénic flow region, the Mach number diverges there; the super-Alfvénic flow is only available in the  $A > 0$  region. Thus,  $A > 0$  in the super-Alfvénic region is a *necessary condition* for trans-magnetosonic accretion/wind solutions. On the other hand, the  $A < 0$  region is the forbidden region on the super-Alfvénic magnetosonic flow solution, where  $M_+^2 < 0$  is obtained.

For the cold MHD flow, we define two characteristic Alfvén Mach numbers related to the Alfvén and fast magnetosonic wave speeds (see [7])

$$M_{\text{AW}}^2(r, \theta) = \alpha, \quad (19)$$

$$M_{\text{FM}}^2(r, \theta) = \alpha + \beta^2. \quad (20)$$

The locations of  $M_\pm^2 = M_{\text{AW}}^2$  and  $M_\pm^2 = M_{\text{FM}}^2$  indicate the Alfvén point and the fast magnetosonic point, respectively. Just on the event horizon, we obtain  $M_{\text{FM}}^2 = 0$ . Figure 1 shows the ingoing and outgoing flow solutions; both solutions are started from the separation surface, which separates the gravitational force dominated region and the centrifugal force dominated region (see [7]), with zero poloidal velocity. These solutions cross the  $M^2 = M_{\text{AW}}^2$  and  $M^2 = M_{\text{FM}}^2$  curves in this order (Fig. 1a), and the  $|u^r| = u_{\text{AW}}^r \equiv \sqrt{\Sigma/\Delta}(B_p^2/4\pi\mu n)\alpha$  and  $|u^r| = u_{\text{FM}}^r \equiv \sqrt{\Sigma/\Delta}(B_p^2/4\pi\mu n)(\alpha + \beta^2)$  curves (Fig. 1b). Because  $\eta = \text{constant}$  through the flow solution, the number density  $n$  diverges at the injection point, where  $u^r = 0$ , so that our definite radial Alfvén wave speed and the fast magnetosonic wave speed become zero,  $(u_{\text{AW}}^r)_{\text{inj}} = (u_{\text{FM}}^r)_{\text{inj}} = 0$ , at the injection point.

Note that the function  $\xi(r, \theta)$  gives the distribution of the cross section of the magnetic flux tube in the poloidal plane. To plot the flow solution as shown in Figure 1, we

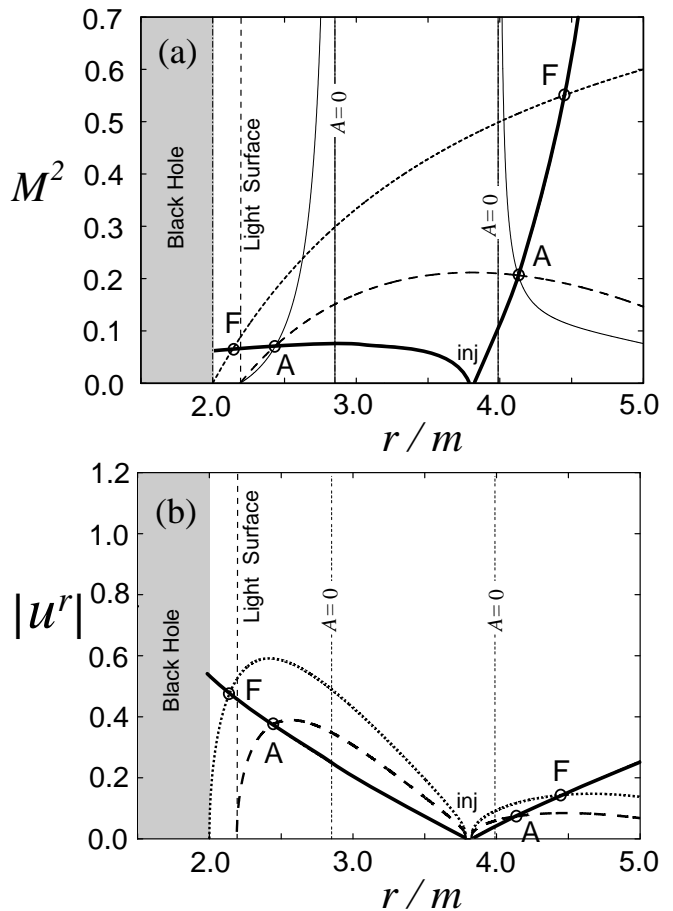


FIG. 1: Transfast magnetosonic inflow and outflow solutions (thick bold curves) started from the separation surface with zero velocity (labeled ‘‘inj’’). (a) The square of the Alfvén Mach number  $M^2$  vs. radius  $r/m$  and (b) the radial 4-velocity of the flow  $u^r$  vs. radius  $r/m$ . The solution is plotted on the equatorial plane ( $\theta = \pi/2$ ) in Schwarzschild geometry ( $a = 0$ ), where the magnetic field configuration is assumed with  $\xi(r, \theta) = 1.0$ . The flow parameters are given as  $\hat{E} = 1.15$ ,  $m\Omega_F = 0.7\Omega_{\text{max}}$ ,  $\hat{L}\Omega_F = 0.6$ , where  $\Omega_{\text{max}}$  is the maximum value of  $\Omega_F$ , and is given as the double roots of  $\alpha = 0$ . (If  $\Omega_F > \Omega_{\text{max}}$ , no light surfaces exist along a magnetic field line considered.) The broken curve shows the  $M^2 = M_{\text{AW}}^2$  curve (left) and the  $|u^r| = u_{\text{AW}}^r$  curve (right), and the dotted curve shows the  $M^2 = M_{\text{FM}}^2$  curve (left) and the  $|u^r| = u_{\text{FM}}^r$  curve (right). The crossing points of these curves with the flow solution labeled by ‘‘A’’ and ‘‘F’’ are the Alfvén and fast magnetosonic points, respectively. The thin curves started from the light surface and approached to the  $A = 0$  line are unphysical solutions of the quadratic equation.

need to specify the stream line of the flow; in Figure 1, the flow streaming along the equatorial plane is plotted, but the magnetic flux tube determined by the function  $\xi$  is not a conical shape. Figure 2 shows the ingoing flow solutions for rapidly rotating Kerr black hole cases. Each inflow enters the event horizon with a finite Mach number (Fig. 2a) or breaks at the  $A = 0$  location (Fig. 2b), where the Mach number of the trans-fast MHD inflow diverges.

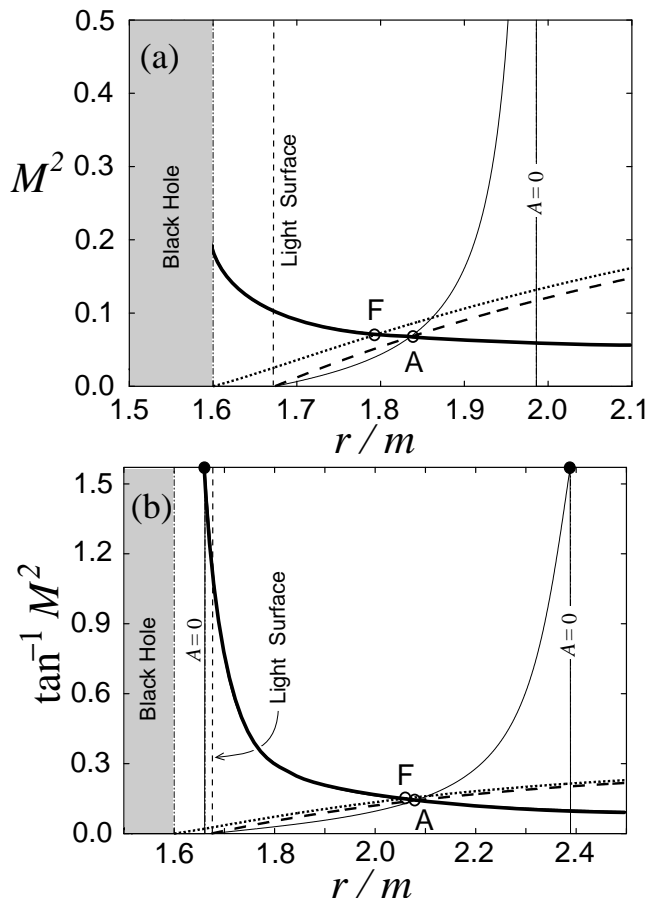


FIG. 2: The square of the Alfvén Mach number  $M^2$  vs. radius  $r/m$  for transfast magnetosonic inflow solutions (*thick bold curve*) on the equatorial plane ( $\theta = \pi/2$ ) in Kerr geometry ( $a = 0.8m$ ). The flow parameters are given as  $\hat{E} = 1.0$ ,  $m\Omega_F = 0.5\Omega_{\max}$ ,  $\hat{L}\Omega_F = -0.5$  (*left*) and  $\hat{L}\Omega_F = 0.09$  (*right*). The magnetic field configuration is assumed by equation (A2) discussed in §A. The right-hand figure shows an *unphysical solution*, where the Alfvén Mach number  $M^2$  diverges at the location of  $A = 0$ . The black spots (*right*) indicate  $M^2 = \infty$ . The dotted curve shows the  $M^2 = M_{\text{AW}}^2$  curve, and the solid curve shows the  $M^2 = M_{\text{FW}}^2$  curve. The crossing points of these curves with the flow solution labeled by “A” and “F” are the Alfvén and fast magnetosonic points, respectively. The thin curves started from the light surface and approached to the  $A = 0$  line are unphysical as inflow solutions.

In Figures 1 and 2, the functions  $\xi(r, \theta)$  are considered as simple models that satisfied conditions specified at some characteristic radii (the details of the conditions will be presented in Appendix A). The general properties of trans-magnetosonic flows discussed here do not depend on detail of the functional form of  $\xi(r, \theta)$ .

The poloidal velocity of a cold MHD flow can be expressed in terms of  $M^2$  and  $\beta^2$  (or  $\xi^2$ ) with the conserved quantities as

$$u_p^2 = \mathcal{B}_p^2 M^4 = \frac{\beta^2 (G_\phi \hat{E} + G_t \hat{L})^2 M^4}{\rho_w^2 (M^2 - \alpha)^2}. \quad (21)$$

When we consider a solution for accretion onto a black hole, we apply  $M^2 = M_-^2$  in the sub-Alfvénic region of  $r > r_A$  and  $M^2 = M_+^2$  in the super-Alfvénic region of  $r < r_A$  (see Fig. 1b). By using the poloidal equation (9), equation (21) can be reduced to

$$u_p^2 = \frac{\hat{e}^2 - \alpha}{\alpha + \beta^2}, \quad (22)$$

which corresponds to a physical trans-Alfvénic accretion solution. From the requirement of  $u_p^2 > 0$ , we find the minimum energy  $\hat{E}_0(r, \theta)$  at each place between the inner and outer light surfaces. The energy  $E$  should be taken as  $E > E_0(r; \Psi)$  along the flow (between the plasma source and the event horizon). Note that, at the location of  $A = 0$  in the super-Alfvénic region (if such a point exists), the poloidal velocity has a finite value, although the Alfvén Mach number diverges. However, the poloidal and toroidal components of the magnetic field vanishes there, while  $\beta$  has a finite non-zero value, as mentioned in the first half of this section.

#### IV. RESTRICTIONS ON MHD FLOWS

##### A. Trans-Alfvénic Flow

Along a magnetic field line  $\Psi(r, \theta) = \text{constant}$ , the location of the Alfvén point ( $r_A, \theta_A$ ) is given by  $M^2 = \alpha$  and

$$\tilde{L}\Omega_F = Y_A \quad (23)$$

with the definition of a function

$$Y \equiv -G_\phi \Omega_F / G_t, \quad (24)$$

where  $\tilde{L} \equiv L/E$ . Although  $\tilde{L}\Omega_F$  is a function of  $\Psi$ , hereafter, we can regard  $\tilde{L}\Omega_F$  as a function of  $r_A$  along the magnetic field line considered; note that  $\theta_A = \theta_A(r_A; \Psi)$ . In the black hole magnetosphere, two surfaces of the Alfvén points (i.e., the Alfvén surfaces) for inflow and outflow are distributed between the inner and outer light surfaces given by the relation  $\alpha = 0$ . For an ingoing MHD flow, the region between the Alfvén surface and the event horizon is the super-Alfvénic region, while the region between the plasma source and the Alfvén surface is the sub-Alfvénic region.

Now, we consider magnetic field line connected to a black hole with a certain value of  $\Omega_F$ . Figures 3a and 3b show the locations of the Alfvén radii for a given  $\tilde{L}\Omega_F$  value. When the magnetic field line rotates faster than the black hole (i.e., a slowly rotating black hole case),  $0 \leq \omega_H \leq \Omega_F$ , whose state is named “type I” in Takahashi et al.[7], the condition for  $\tilde{L}\Omega_F$  for the existence of the Alfvén point in the flow solution is  $(\tilde{L}\Omega_F)_{\min} < \tilde{L}\Omega_F \leq 1$  (see Fig.3a), where  $(\tilde{L}\Omega_F)_{\min}$  is the minimum value of  $\tilde{L}\Omega_F$  for the Alfvén point to appear on the flow, and it is

given by  $dY_A/dr_A = 0$ . The MHD flow with  $E > 0$  and  $L > 0$  only is obtained.

For the type I case, it is possible to select the inner or outer Alfvén point in an accretion solution, and then trans-Alfvénic accretion solutions with two types are acceptable (see [11]); that is, “magneto-like” and “hydro-like” accretion solutions. The magneto-like accretion solution passes through the *inner* Alfvén point and the inner fast magnetosonic point, and the hydro-like accretion solution passes through the *outer* Alfvén point and the middle fast magnetosonic point. Note that, in the latter type solution case, the acceptable range of  $\tilde{L}\Omega_F$  is modified to  $(\tilde{L}\Omega_F)_{\min} < \tilde{L}\Omega_F \leq (\tilde{L}\Omega_F)_{\max}$ , where  $(\tilde{L}\Omega_F)_{\max}$  is the maximum value of  $\tilde{L}\Omega_F$  to avoid the forbidden region discussed in [7] between the outer Alfvén point and the event horizon, and is given by  $dk_A/dr_A = 0$  with  $k_A = 0$ . For a counterrotating case  $a\Omega_F < 0$  (named “type III”), we see the similar restrictions on  $\tilde{L}\Omega_F$  as type I, although we obtain  $L < 0$  and  $E > 0$  flows.

Figure 3b shows the rapidly rotating black hole case of  $0 < \Omega_F < \omega_H$  (named “type II”). For a certain  $\tilde{L}\Omega_F$  value, one Alfvén point is obtained on the flow solution. In this case, the negative energy accretion with  $E < 0$  and  $L < 0$  is possible when  $\tilde{L}\Omega_F \geq 1$ . The flow with

$E > 0$  and  $L \leq 0$  is realized when  $\tilde{L}\Omega_F \leq 0$ . For  $0 < \tilde{L}\Omega_F \leq (\tilde{L}\Omega_F)_{\max}$ , the inflow with  $E > 0$  and  $L > 0$  is realized. More detail discussions about the restriction by the Alfvén points are presented by Takahashi et al.[7].

## B. Super-Alfvénic Flow

After passing through the Alfvén point, the ingoing/outgoing flow solution passes through the fast magnetosonic point automatically. However, if the location of  $A(r; \Psi) = 0$  appears on the flow solution considered in the super-Alfvénic region, the Mach number of this super-fast magnetosonic flow solution diverges there; that is, no physical MHD accretion/wind solution exists. To obtain a physical MHD accretion/wind solution, no  $A = 0$  surfaces in the super-Alfvénic region must be required. Although the value of  $A$  depends on the flow parameters  $\Omega_F$ ,  $E$  and  $L$  under a given function  $\xi(r, \theta)$  and the hole’s spin  $a$ , we will find restrictions on these combinations of parameters to avoid the appearance of the  $A = 0$  location.

The condition  $A > 0$  for a super-Alfvénic flow can be reduced to

$$A(r; \Psi) = \frac{-G_t(1+Y+X)\hat{E}^2}{(G_\phi\Omega_F)^2} \left[ \tilde{L}\Omega_F - (\tilde{L}\Omega_F)^+ \right] \left[ \tilde{L}\Omega_F - (\tilde{L}\Omega_F)^- \right] > 0 \quad (25)$$

with

$$(\tilde{L}\Omega_F)^\pm \equiv \frac{Y}{1+Y+X} \left\{ (1+X) \pm \epsilon \left[ 1 + (1-Y)X - (1+Y+X)\frac{G_t}{\hat{E}^2} \right]^{1/2} \right\}, \quad (26)$$

where  $X \equiv g_{\phi\phi}G_t(1-\xi^2)/\rho_w^2$  and  $\epsilon \equiv \Omega_F(\Omega_F - \omega)/|\Omega_F(\Omega_F - \omega)|$ . When the function  $\xi^2 = \xi^2(r; \Psi)$  is specified as a given magnetic field structure with the field aligned flow parameters  $\Omega_F$  and  $\hat{E}$ , the value of  $(\tilde{L}\Omega_F)^\pm$  is determined along the stream line. In Figures 3c and 3d we show the  $\tilde{L}\Omega_F = (\tilde{L}\Omega_F)^\pm$  curves for the slowly and rapidly rotating black hole cases, respectively. The models of  $\xi^2(r; \Psi)$  are discussed in Appendix A.

To obtain a trans-fast magnetosonic accreting flow onto a black hole, the  $\tilde{L}\Omega_F = \text{constant}$  line must not cross the  $\tilde{L}\Omega_F = (\tilde{L}\Omega_F)^\pm$  curves between the Alfvén point and the event horizon on the  $\tilde{L}\Omega_F - r$  plane. The condition  $A > 0$  for the super-Alfvénic flow solution is satisfied when

$$(i) \quad (\tilde{L}\Omega_F)^- < \tilde{L}\Omega_F < (\tilde{L}\Omega_F)^+$$

in the  $G_t(1+Y+X) > 0$  region, and

$$(ii) \quad \tilde{L}\Omega_F < (\tilde{L}\Omega_F)^+ \text{ or } \tilde{L}\Omega_F > (\tilde{L}\Omega_F)^-$$

in the  $G_t(1+Y+X) < 0$  region. The value of  $(\tilde{L}\Omega_F)^-$  diverges at the location of  $X = -(1+Y)$ , while  $(\tilde{L}\Omega_F)^+$  has a non-zero finite value there. Thus, the value of  $\tilde{L}\Omega_F$  (or the location of the Alfvén point) is restricted. Examples of this restriction on  $\tilde{L}\Omega_F$  for the  $A > 0$  regions are also shown in Figures 3c and 3d for Type I and II cases, respectively. For accretion onto a slowly rotating black hole (type I; see Fig. 3c), we see that the case (i) is applied everywhere. For type I and III, the location of  $X = -(1+Y)$  may exist, although it depends on a model of  $\xi^2$ ; that is, the case (ii) may arise. In this case, however, there is no additional restriction in the  $(\tilde{L}\Omega_F)_{\min} < \tilde{L}\Omega_F < 1$  range. On the other hand, the case (ii) arises near the event horizon for a rapidly rotating black hole case (type II; see Fig. 3d). Note that for type II the case (i) is also possible just outside the event horizon, although it depends on  $\xi$  (to be discussed in § V A). In this case, the negative energy inflow solutions only are obtained; the positive energy inflow solutions

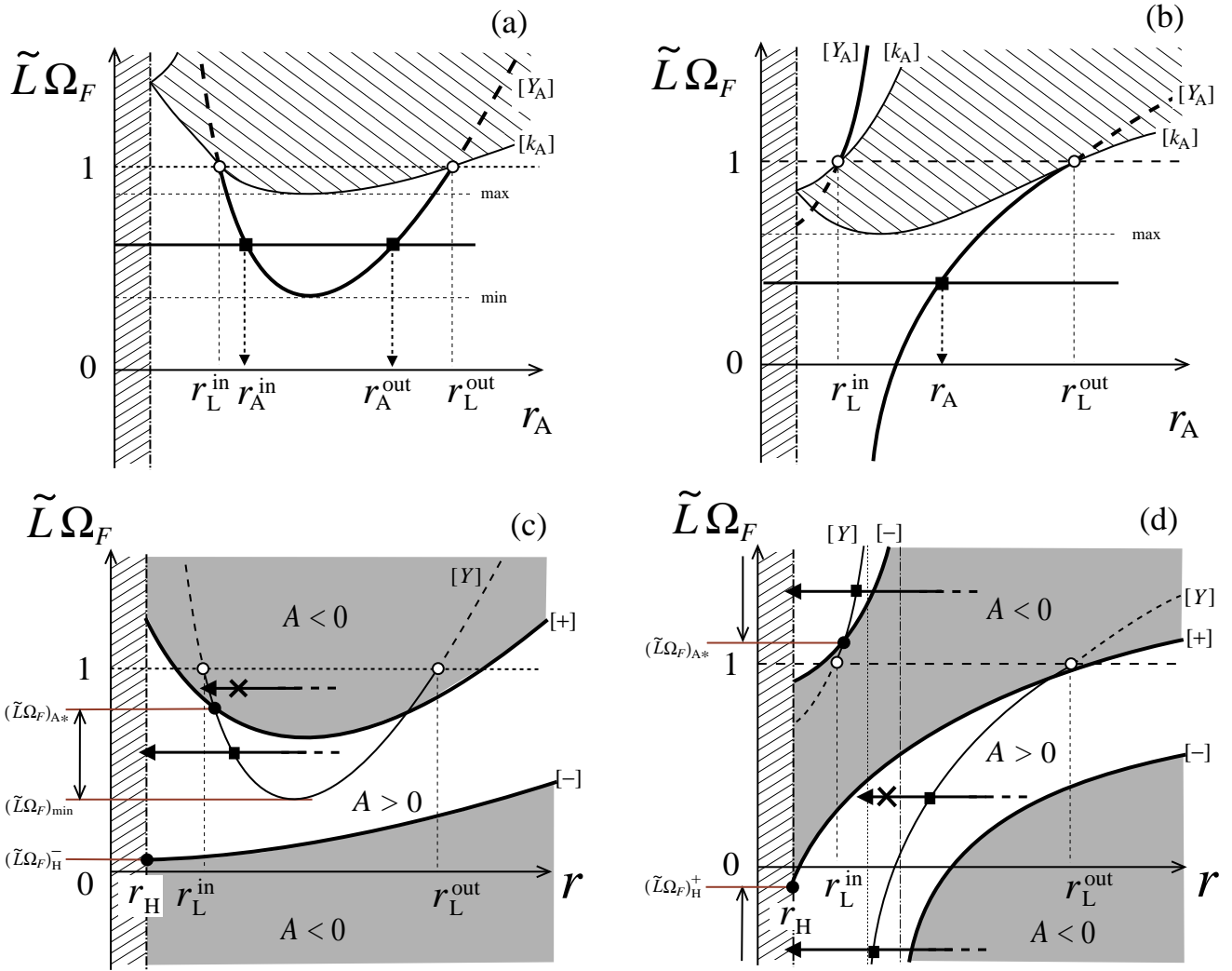


FIG. 3: (TOP) The possible range of  $\tilde{\Omega}_F$  for (a) type I and (b) type II cases. The vertical axis is  $\tilde{\Omega}_F$ , while the horizontal axis is the Alfvén radius. Curves  $\tilde{\Omega}_F = Y(r_A)$  (marked by  $[Y_A]$ ) and  $k(r_A) = 0$  (marked by  $[k_A]$ ) are plotted. Two crossing points between the  $\tilde{\Omega}_F = Y(r_A)$  curve and  $\tilde{\Omega}_F = \text{constant}$  line in the type I case (left) show the inner and outer Alfvén radii. On the other hand, one Alfvén radius exists in the type II case (right). The hatched region bounded by  $k_A = 0$  shows the forbidden region for the parameter. For type I case the range of  $(\tilde{\Omega}_F)_{\min} < \tilde{\Omega}_F < 1$  is acceptable as a trans-Alfvénic solution, while for type II case the ranges of  $\tilde{\Omega}_F < (\tilde{\Omega}_F)_{\max}$  and  $1 < \tilde{\Omega}_F$  are acceptable. (BOTTOM) Curves  $\tilde{\Omega}_F = (\tilde{\Omega}_F)^\pm$  (marked by  $[+]$  and  $[-]$ ) and  $\tilde{\Omega}_F = Y$  (marked by  $[Y]$ ) for (c) type I and (d) type II cases. Some accretion solutions with certain  $\tilde{\Omega}_F$  values are shown by horizontal arrows, where the crossing point with the  $\tilde{\Omega}_F = Y$  curve (i.e.,  $Y = Y_A$ ) indicates the Alfvén point (marked by the fill square). When the solution crosses the  $\tilde{\Omega}_F = (\tilde{\Omega}_F)^\pm$  curve, where  $A = 0$ , the Mach number of the solution diverges there; that is, no physical accretion solution exists (the horizontal arrow marked by the cross). The shaded regions show the  $A < 0$  regions. Note that the  $k > 0$  region is enclosed in the  $A < 0$  region. In these schematic diagrams, we set up the field configuration  $\xi^2$  by equation (A1) for type I and equation (A2) for type II near the equator as typical models.

are forbidden because the  $A < 0$  region appears on the way to the horizon.

In the last of this section, we should mention that there is the innermost limit of the inner Alfvén point (labeled by “A\*” in Figs. 3c and 3d) under the given parameters  $\Omega_F$  and  $\hat{E}$ . This limit gives the restriction on the  $\tilde{\Omega}_F$  value, which is the maximum value for type I case and the minimum value for type II case. The details are discussed in Appendix B.

## V. BOUNDARY CONDITIONS AT THE EVENT HORIZON

### A. Inclination of Magnetic Field Lines

Without the trans-field equation and the informations for the plasma sources (as the initial conditions for MHD flows), we can not obtain the concrete function of  $\xi(r, \theta)$  in the black hole magnetosphere considered. Neverthe-



less, just on the event horizon, we have already known that  $\xi_H = 1$  (or  $\beta_H^2 = -\alpha_H$ ), which is the boundary condition at the horizon. However, just outside the event horizon, the magnetic field configuration depends on the plasma inertia effects. Here, we discuss the function  $\xi^2(r, \theta)$  near the event horizon. One may expect that the signature of the function  $A_H(\theta) \equiv A(r_H, \theta)$  is at least determined for any field aligned flow parameter sets. However, at the event horizon, the value of the function  $X$  in equation (25) can not be specified by only the condition  $\xi_H^2 = 1$ . Now, we will expand the function  $\xi^2$  as  $\xi^2 = 1 + \chi(r/r_H - 1)$ , where  $\chi \equiv r_H(\partial_r \xi)_H$  represents the magnetic field configuration near the horizon. To obtain physical MHD accretion solutions satisfying the condition  $A_H > 0$ , we should discuss the restrictions on the value of  $\chi$  and on the allowable ranges of the field aligned flow parameters (e.g.,  $E$ ,  $L$  and  $\Omega_F$ ), which should be consistent with the boundary condition at the plasma sources. Note that the function  $\chi$  can be expressed as the differentials of  $\mathcal{B}_p^2$  and  $\mathcal{B}_\phi^2$  at the event horizon.

The restrictions on the function  $\chi(\theta)$  specify how the inclination angles change (having poloidal and toroidal components) going away from the horizon. In other words, the  $\chi$  value represents the deviation of the inclination (or pitch) angle at the horizon from the  $\xi^2(r, \theta) = 1$

model. To consider this situation, we also expand the magnetic field components as  $\mathcal{B}_p = \mathcal{B}_{pH} + \delta\mathcal{B}_{pH}(r/r_H - 1)$  and  $\mathcal{B}_\phi = \mathcal{B}_{\phi H} + \delta\mathcal{B}_{\phi H}(r/r_H - 1)$ . Then, we obtain

$$\left(\frac{\mathcal{B}_p}{\mathcal{B}_\phi}\right)^2 = \frac{1}{(-\alpha_H)} \left[ 1 + 2 \left( \frac{\delta\mathcal{B}_p}{\mathcal{B}_p} - \frac{\delta\mathcal{B}_\phi}{\mathcal{B}_\phi} \right)_H \left( \frac{r}{r_H} - 1 \right) \right]. \quad (27)$$

When we modify the magnetic field configuration  $(\delta\mathcal{B}_p/\mathcal{B}_p)_H > 0$  and/or  $(\delta\mathcal{B}_\phi/\mathcal{B}_\phi)_H < 0$ , we see that the value of  $\chi$  increases. Although the term  $\mathcal{B}_p$  means the divergence of the magnetic flux tube to the  $(+r)$ -direction, when the ratio of the divergence  $(\delta\mathcal{B}_p/\mathcal{B}_p)_H$  for a certain model is larger than that of the  $\xi^2 = 1$  ( $\chi = 0$ ) model, we see that  $(\delta\mathcal{B}_p/\mathcal{B}_p)_H > 0$ . Furthermore, if the bending angle to the toroidal direction is smaller than that in the force-free case ( $\delta\mathcal{B}_\phi = 0$  along a magnetic field line), we see that  $(\delta\mathcal{B}_\phi/\mathcal{B}_\phi)_H < 0$ .

If the location of  $A = 0$  appears between the Alfvén point and the event horizon (i.e., the super-Alfvénic region of the flow), such a solution is unphysical as an accretion solution as mentioned in § IV B. At the event horizon, to accrete onto the black hole, the condition  $A_H(\chi) > 0$  must be required. The boundaries of the  $A_H(\chi) > 0$  region on the  $\chi$ - $\tilde{L}\Omega_F$  plane are obtained by

$$(\tilde{L}\Omega_F)_H^\pm(\chi) = \frac{\Omega_F}{\Omega_F + \omega_H + \omega_H X_H} \left\{ (1 + X_H) \pm \epsilon_H \left[ 1 + \left( \frac{\Omega_F^2 - \omega_H^2}{\omega_H^2} \right) \frac{g_{tt}^H}{\tilde{E}^2} - \left( \frac{\Omega_F - \omega_H}{\omega_H} \right) \left( 1 - \frac{g_{tt}^H}{\tilde{E}^2} \right) X_H \right]^{1/2} \right\}, \quad (28)$$

where  $\epsilon_H \equiv \Omega_F(\Omega_F - \omega_H)/|\Omega_F(\Omega_F - \omega_H)|$ ,  $X_H \equiv X(r_H) = \mathcal{H}\chi$  and  $\mathcal{H} \equiv 2m^2 r_H G_t^H / [(r_H - m)\Sigma_H]$ . Figure 4 shows the relation between  $(\tilde{L}\Omega_F)_H^\pm$  and  $\chi$  for type I and II cases. There is a maximum  $\chi$  value ( $\equiv \chi_{\max}$ ) for existing  $A > 0$  region in both type I and II cases.

The value of  $(\tilde{L}\Omega_F)_H^-$  becomes zero at  $\chi = \chi_0$ , and diverges at  $\chi = \chi_\infty$ . Although these characteristic  $\chi$ 's depend on the flow parameters, the details are discussed in Appendix C. Furthermore, the relations between the  $\chi$  value and the acceptable ranges of  $\tilde{L}\Omega_F$  are also summarized there.

## B. Black Hole Spin-Up/Down via MHD Accretion

In § IV B and § V A (see also Appendix C), we have discussed the restriction on  $L/E$  for the MHD accretion onto a black hole to avoid the  $A = 0$  surface on the flow solution, by considering the conditions at both the event horizon and the Alfvén point. Here, we will discuss the increase or decrease of the angular velocity (spin-up/down) of a rotating black hole by applying this restriction on  $L/E$  to equation (1). Hereafter, we treat

the case of  $a > 0$  and  $\Omega_F > 0$  mainly (i.e., type I and II cases).

Although the accreting gas carries the mass and angular momentum into the black hole, both the cases  $\delta\omega_H/\omega_H > 0$  (spin-up) and  $\delta\omega_H/\omega_H < 0$  (spin-down) are possible for the positive energy ( $E > 0$ ) MHD inflows. That is, the range of  $\tilde{L}\Omega_F > (\tilde{L}\Omega_F)_\omega$  gives the hole's spin-up and the range of  $\tilde{L}\Omega_F < (\tilde{L}\Omega_F)_\omega$  gives the spin-down, where

$$(\tilde{L}\Omega_F)_\omega \equiv (1 + r_H/m) a\Omega_F; \quad (29)$$

in Figure 4 we show the  $\tilde{L}\Omega_F = (\tilde{L}\Omega_F)_\omega$  line (where  $\delta\omega_H = 0$ ). [Similarly, with respect to the spin parameter  $a$ , we see that  $\delta(a/m) > 0$  (or  $\delta(a/m) < 0$ ) for positive energy MHD inflows with  $\tilde{L}\Omega_F > 2a\Omega_F$  (or  $\tilde{L}\Omega_F < 2a\Omega_F$ ).] Furthermore, by considering the restrictions from the Alfvén point and the event horizon, we obtain that increase of the angular velocity of the black hole  $\delta\omega_H > 0$  by MHD inflows is realized when  $(\tilde{L}\Omega_F)_\omega < \tilde{L}\Omega_F < (\tilde{L}\Omega_F)_{A*}$  for type I case, and  $(\tilde{L}\Omega_F)_\omega < \tilde{L}\Omega_F < (\tilde{L}\Omega_F)_H^+$  for type II case. Note that, even if positive angular momentum  $L > 0$  of MHD flow falls into the black hole, the angular velocity of the black

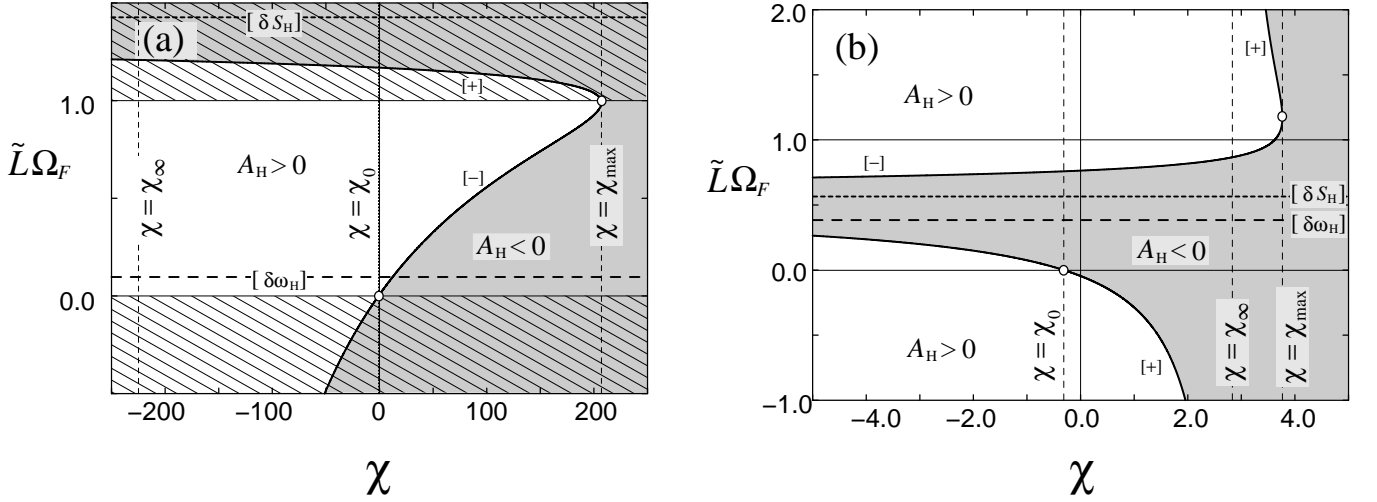


FIG. 4: The horizon's boundary condition on  $\tilde{\Omega}_F$  for (a) type I of  $a = 0.3m$  and (b) type II of  $a = 0.9m$ . The bold thick curves denote the  $\tilde{\Omega}_F = (\tilde{\Omega}_F)_H^\pm(\chi)$  curves (marked [+] and [-] respectively) with  $\hat{E}^2 = 1.0$ ,  $\Omega_F = 0.5\Omega_{\max} = 0.09623/m$  and  $\theta = \pi/2$ . The shaded region corresponds to the  $A_H < 0$  region, which is forbidden as a black hole accretion solution. The hatched regions in (a) show the  $\tilde{\Omega}_F > 1$  and  $\tilde{\Omega}_F < 0$  regions (unphysical). The  $\tilde{\Omega}_F = Y_H$  line is denoted by the dotted line and labeled by  $[\delta S_H]$ . The horizontal broken line marked by  $[\delta\omega_H]$  shows the  $\tilde{\Omega}_F = (\tilde{\Omega}_F)_\omega$  line. Although, in (b), it seems  $(\tilde{\Omega}_F)_H^+ < (\tilde{\Omega}_F)_\omega < (\tilde{\Omega}_F)_H^-$  in this plot, we can find the case  $(\tilde{\Omega}_F)_\omega < (\tilde{\Omega}_F)_H^+ < Y_H$  for larger ( $-\chi$ ) values. For the range  $(\tilde{\Omega}_F)_\omega < \tilde{\Omega}_F < (\tilde{\Omega}_F)_H^+$ , the spin-up is caused for type II.

hole can be decreased; that is,  $\delta\omega_H < 0$  is obtained for  $0 < \tilde{\Omega}_F < (\tilde{\Omega}_F)_\omega$ .

For a slowly rotating black hole of type I case, equatorial (low-latitude) inflows onto the black hole contribute to the spin-up, but spin-down effects can be also realized by MHD plasma accreting from the polar (higher latitude) region of the event horizon. The value of  $(\tilde{\Omega}_F)_{\min}$  can be specified by the latitude of the Alfvén point, where  $r_A(\theta_A) = r_A^{\text{in}} = r_A^{\text{out}}$ , so that we define the critical angle of  $\theta_A [\equiv (\theta_A)_{\text{cr}}]$  by  $(\tilde{\Omega}_F)_{\min} = (\tilde{\Omega}_F)_\omega$ , except for a Schwarzschild black hole, where  $(\tilde{\Omega}_F)_\omega$  becomes zero. When  $\theta_A > (\theta_A)_{\text{cr}}$  along a flow considered, the relation of  $\tilde{\Omega}_F = (\tilde{\Omega}_F)_{\min} > (\tilde{\Omega}_F)_\omega$  is satisfied and the MHD inflows only contribute to the spin-up of the black hole. On the other hand, when  $\theta_A < (\theta_A)_{\text{cr}}$ , the situation  $(\tilde{\Omega}_F)_{\min} < \tilde{\Omega}_F < (\tilde{\Omega}_F)_\omega$  (the black hole's spin-down) is also possible; note that, even if  $\theta_A < (\theta_A)_{\text{cr}}$ , the MHD inflows in the range of  $(\tilde{\Omega}_F)_\omega < \tilde{\Omega}_F < (\tilde{\Omega}_F)_{A^*}$  can lead the black hole into the spin-up. For larger values of  $a$  or for smaller values of  $\Omega_F$ , such a spin-down range specified by the critical value angle  $(\theta_A)_{\text{cr}}$  expands toward lower latitude regions, while the value of  $(\tilde{\Omega}_F)_\omega$  increases; in the  $a \rightarrow M$  limit, we see that  $(\tilde{\Omega}_F)_\omega \rightarrow Y_H = \Omega_F/\omega_H (> 1)$ . Thus, the spin-down effect dominates for a rapidly rotating black hole of type I; that is, even if  $\Omega_F > \omega_H$ , the MHD inflows spin down the hole's rotation.

For a rapidly rotating black hole of type II case, both  $L > 0$  and  $L < 0$  inflows are possible. The inflow with  $L > 0$  decreases the spin of the black hole when  $0 < \tilde{\Omega}_F < (\tilde{\Omega}_F)_\omega$ . On the other hand, the  $L > 0$

inflows increase the hole's spin when  $(\tilde{\Omega}_F)_\omega < \tilde{\Omega}_F < (\tilde{\Omega}_F)_H^+$ . However, after the black hole spin-up, the value of  $(\tilde{\Omega}_F)_\omega$  increases, so that the parameter range of  $\tilde{\Omega}_F$  for the spin-up decreases. Note that, in the  $a \rightarrow m$  limit, any ingoing flows with  $L > 0$  cannot increase the angular velocity and the spin parameter of the black hole no more, because both  $(\tilde{\Omega}_F)_\omega$  and  $2a\Omega_F$  become  $Y_H$ , where  $(\tilde{\Omega}_F)_H^+ < Y_H < (\tilde{\Omega}_F)_H^-$ ; that is the  $A_H > 0$  region. On the other hand, in type II case, the negative angular momentum MHD inflows are also possible. In such a case, we always obtain  $\delta\omega_H < 0$  and  $\delta(a/m) < 0$  as expected. Furthermore, if we consider the negative energy ( $E < 0$ ) MHD inflows [7], which always carry the negative angular momentum ( $L < 0$ ), we always see that  $\delta\omega_H/\omega_H < 0$  and  $\delta(a/m) < 0$ .

Figure 5 shows the summary of the hole's spin-up/down by MHD inflows, which also includes the contribution by the magnetic field parameter  $\chi$ . First, in the case of type I (see Fig. 5a), the spin-up of  $\delta\omega_H/\omega_H > 0$  is obtained when the value of  $\tilde{\Omega}_F$  is in the range of  $\text{MAX}[(\tilde{\Omega}_F)_{\min}, (\tilde{\Omega}_F)_\omega, (\tilde{\Omega}_F)_H^-] < \tilde{\Omega}_F < (\tilde{\Omega}_F)_{A^*} < 1$ . The spin-down of  $\delta\omega_H/\omega_H < 0$  is obtained when  $\text{MAX}[(\tilde{\Omega}_F)_{\min}, (\tilde{\Omega}_F)_H^-] < \tilde{\Omega}_F < (\tilde{\Omega}_F)_\omega$ , which is only realized for inflows with  $\theta_A < (\theta_A)_{\text{cr}}$ . Next, for type II case (see Fig. 5b), we obtain the spin-up of  $\delta\omega_H/\omega_H > 0$  when  $(\tilde{\Omega}_F)_\omega < \tilde{\Omega}_F < (\tilde{\Omega}_F)_H^+$  for  $\chi < \chi_\omega$ , where  $\chi_\omega$  is defined by the condition of  $(\tilde{\Omega}_F)_H^+ = (\tilde{\Omega}_F)_\omega$ . The spin-down of  $\delta\omega_H/\omega_H < 0$  is obtained when (1)  $\tilde{\Omega}_F < \text{MIN}[(\tilde{\Omega}_F)_\omega, (\tilde{\Omega}_F)_H^+]$  or  $(\tilde{\Omega}_F)_{A^*} < \tilde{\Omega}_F$  for  $\chi < \chi_\infty$  and (2)  $(\tilde{\Omega}_F)_{A^*} < \tilde{\Omega}_F < (\tilde{\Omega}_F)_H^+$  for  $\chi_\infty < \chi < \chi_{\max}$ . When we consider a coun-

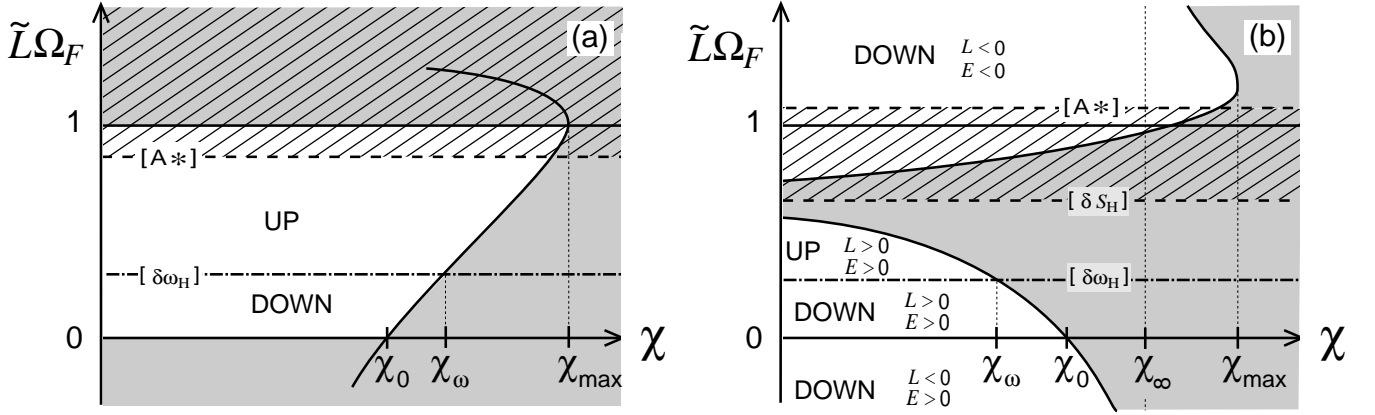


FIG. 5: Summary of the  $\tilde{L}\Omega_F$  ranges for the spin-up/down of a black hole in (a) type I case and (b) type II case. The value of  $\tilde{L}\Omega_F$  for acceptable MHD accretion is restricted by at least the boundary condition at the event horizon ( $A_H > 0$ ) and the condition of the Alfvén point for existing in the  $A > 0$  region. The shaded forbidden region is the same as that of Fig. 4. The labels  $[A*]$ ,  $[\delta\omega_H]$  and  $[\delta S_H]$  show the  $\tilde{L}\Omega_F = (\tilde{L}\Omega_F)_{A*}$  line, the  $\tilde{L}\Omega_F = (\tilde{L}\Omega_F)_\omega$  line and the  $\tilde{L}\Omega_F = Y_H$  line, respectively. The hatched region is forbidden by the condition at the Alfvén point. For type I case, the range of  $(\tilde{L}\Omega_F)_{\min} < \tilde{L}\Omega_F < (\tilde{L}\Omega_F)_{A*}$  is acceptable, and the MHD inflows with  $\theta_A > (\theta_A)_{\text{cr}}$  always cause the hole's spin-up.

terrotating magnetosphere of  $\Omega_F < 0$  (type III), where  $a > 0$  is considered, we have the relation  $\tilde{L}\Omega_F > 0 > 2a\Omega_F > (\tilde{L}\Omega_F)_\omega$ . In this type III case, both the angular momentum and the spin parameter of the black hole decrease; that is,  $\delta\omega_H/\omega_H < 0$  and  $\delta(a/m) < 0$ .

From the definition of the surface area of the black hole  $S_H \equiv 4\pi(r_H^2 + a^2)$ , we obtain the relation  $\delta S_H \propto E - \omega_H L$ . Here, we should remember that, in the case of type II, the acceptable range of  $\tilde{L}\Omega_F$  for positive energy ( $E > 0$ ) MHD inflows is given as  $\tilde{L}\Omega_F < (\tilde{L}\Omega_F)_H^+ \leq Y_H$ , while  $\tilde{L}\Omega_F < 1 < Y_H$  in the case of type I and  $\tilde{L}\Omega_F > 0 > Y_H$  in the case of type III. So, for  $E > 0$  flows (in all cases of types I, II and III), we can show  $\delta S_H > 0$ , which means the increasing surface area of a black hole. On the other hand, for  $E < 0$  flows (that can be possible in the case of type II), the relation of  $Y_H < \tilde{L}\Omega$  is always satisfied, and then the relation of  $\delta S_H > 0$  is also satisfied. Thus, the area law  $\delta S_H > 0$  of the black hole is confirmed for stationary and axisymmetric ideal MHD accretion flows.

### C. Secular Evolution of the Black Hole Spin

In § V B, we mentioned that the MHD inflow prevents the evolution to the maximally rotating black hole. This is because  $\delta\omega_H < 0$  and  $\delta(a/m) < 0$  for the extreme rotating black hole limit. On the other hand, we know that  $\delta\omega_H > 0$  and  $\delta(a/m) > 0$  for the non-rotating black hole case. Now, we will discuss a secular evolution of the black hole spin by MHD accretion. Here, we assume that the values of  $L(\Psi)$ ,  $E(\Psi)$  and  $\Omega_F(\Psi)$  keep constants for a magnetic flux tube considered (a  $\Psi = \text{constant}$  line) during the evolution. Furthermore, we do not discuss the plausible configuration of the magnetic field as a global

solution of the black hole magnetosphere.

First, we consider the case of type I ( $0 < \omega_H < \Omega_F$ ). When the magnetized plasma of  $(\tilde{L}\Omega_F)_\omega < \tilde{L}\Omega_F < (\tilde{L}\Omega_F)_{A*}$  falls into the black hole, the spin of the black hole will increase in secular time-scale. Then, the value of  $(\tilde{L}\Omega_F)_\omega$  also increases, and the state of  $\tilde{L}\Omega_F = (\tilde{L}\Omega_F)_\omega$ , where  $\delta\omega_H = 0$ , will be realized sometime. In this state, the evolution of the black hole's spin is terminated. On the other hand, when  $(\tilde{L}\Omega_F)_{\min} < \tilde{L}\Omega_F < (\tilde{L}\Omega_F)_\omega$ , the black hole's spin decreases, and the value of  $(\tilde{L}\Omega_F)_\omega$  is also decreases. The final state will be settled to  $\tilde{L}\Omega_F = (\tilde{L}\Omega_F)_\omega$ . Although the spin value  $a$  terminated by accreting MHD plasma is given by  $(\tilde{L}\Omega_F)_\omega = \tilde{L}\Omega_F$ , the values of  $L$ ,  $E$  and  $\Omega_F$  should be specified by a magnetized accretion disk model. Note that, during the spin-up stage, the situation of  $\omega_H \rightarrow \Omega_F$  may be realized before the  $\tilde{L}\Omega_F = (\tilde{L}\Omega_F)_\omega$  state. In this case, the spin value  $a$  terminated is specified by  $\Omega_F$ .

Next, we consider the type II case ( $0 < \Omega_F < \omega_H$ ). When magnetized plasma with  $(\tilde{L}\Omega_F)_\omega < \tilde{L}\Omega_F < (\tilde{L}\Omega_F)_H^+$ , the black hole will spin up in secular time scale. In this case, the value of  $(\tilde{L}\Omega_F)_\omega$  also increases and the situation of  $\tilde{L}\Omega_F = (\tilde{L}\Omega_F)_\omega$  would be realized. When  $0 < \tilde{L}\Omega_F < (\tilde{L}\Omega_F)_\omega$ , the black hole spins down in spite of the positive angular momentum inflows. With decreasing the hole's spin, the value of  $(\tilde{L}\Omega_F)_\omega$  also decreases, and the state of  $\tilde{L}\Omega_F = (\tilde{L}\Omega_F)_\omega$  would be realized. One may expect that, by decreasing the angular velocity of the black hole, the state of  $\omega_H \rightarrow \Omega_F$  is achieved before reaching the state of  $\tilde{L}\Omega_F = (\tilde{L}\Omega_F)_\omega$ . However, the state of  $\omega_H \rightarrow \Omega_F$  is only possible for the  $L < 0$  inflows (see Appendix C). So that, the inflows with  $L > 0$  are terminated to the state of  $\tilde{L}\Omega_F = (\tilde{L}\Omega_F)_\omega$ . In type II case, the negative angular momentum inflows are possible when

$\tilde{L}\Omega_F < 0$  or  $\tilde{L}\Omega_F > (\tilde{L}\Omega_F)_{A*}$ . The rotating black hole spins down, and reaches the state  $\omega_H \rightarrow \Omega_F$ . For the magnetically dominated accretion flows, where  $E < 0$  and  $L < 0$ , such a state would be only realized after a long time spin evolution. Although the state  $\omega_H \rightarrow \Omega_F$  can be achieved in both type I and II, the transition from type I to type II or the reverse is impossible. This is because the asymptotic evolution  $\omega_H \rightarrow \Omega_F$  is possible for  $L > 0$  inflows of type I or for  $L < 0$  inflows of type II. The transition between type I and II contradicts the model's assumption that the field-aligned parameters do not change during the hole's evolution.

In this section, we have discussed about the spin-up/down effects along *one* magnetic flux tube. However, in actual black hole magnetosphere models, the above arguments could be considered for each magnetic flux, and the effects on the black hole spin should be integrated over the whole magnetic fluxes across the event horizon. In type I case, although the equatorial inflow would dominate in the black hole accretion and such an inflow contributes to the spin-up, but the spin-down by the inflow in the polar region may not be negligible in a black hole magnetosphere. We must consider the spin-down effect carefully in such a case. In the polar region, the state  $(\tilde{L}\Omega_F)_{\min} < (\tilde{L}\Omega_F)_\omega$  is easily obtained except for a non-rotating black hole case. Then, the ingoing flows can carry the energy into the black hole with less angular momentum; this means the spin-down of the black hole. When disk's gases fall into the black hole along the disk-black hole connected dipole-like magnetic field lines [12, 15], such a situation would be possible. Thus, the configuration of the magnetic field would be very important in astrophysical situations. To estimate the actual spin-up/down of the black hole, we need to integrate the spin-up/down effects on each magnetic flux tube from the pole to the equator. To do this, it is necessary to construct a reasonable model of magnetized accretion disk for distributions  $E = E(\theta_H)$ ,  $L = L(\theta_H)$ ,  $\Omega_F = \Omega_F(\theta_H)$  and  $\eta = \eta(\theta_H)$ . Furthermore, the function  $\chi = \chi(\theta_H)$  over the event horizon should be obtained from the studies of the GS equation around the event horizon. Then, we can estimate the evolution of the rotating black hole. However, this problem remains as our future task.

## VI. CONCLUDING REMARKS

We have discussed about stationary and axisymmetric ideal MHD inflows onto a black hole. We have shown that a *non-singular* distribution of  $\beta(r, \theta)$  gives ingoing and/or outgoing trans-magnetosonic flow solutions without critical behavior. Such solutions automatically satisfy the regularity conditions at the magnetosonic point, and passes through the magnetosonic point. In a cold flow case, we only solve the quadratic equation for  $M^2$  to obtain trans-fast magnetosonic flow solutions. The ingoing flow passes through the inner or middle fast magnetosonic point. When we consider a hot MHD flow, we

can also treat the flow solution as a polynomial of high degree in  $M^2$  without the regularity condition at the fast and slow magnetosonic points.

In this paper, to discuss cold MHD inflows onto a black hole, we have not specified the function  $\beta$  (or  $\xi$ ) without the GS equation. However, we have found the restrictions on the field-aligned flow parameters under a given field geometry. The ranges of possible  $\tilde{L}\Omega_F$  values for black hole accretion are restricted by the condition at the Alfvén point as discussed in § IV A and Appendix B and by the condition  $A(r; \Psi) > 0$  along the magnetic stream function that is discussed in § IV B, where the function  $A$  depends on the MHD flow energy  $E$ , the field geometry  $\xi$  (or  $\beta$ ), and the angular momentum related parameter  $\tilde{L}\Omega_F$ . Although the value of  $\tilde{L}\Omega_F$  is related to the energy and angular momentum of the ingoing flow, the field geometry around the event horizon restricts these values. Furthermore, we have discussed the inclination  $\chi$  of magnetic field lines at the event horizon. When we try to solve the magnetic field distribution from the plasma source to the event horizon in a black hole magnetosphere, we should be aware of this boundary condition. Note that the restrictions and conditions discussed in this paper are model independent as we are focusing on stationary and axisymmetric black hole ideal MHD accretion. In future studies of black hole magnetospheres (including numerical studies), our approach will be helpful to check the magnetic field structure near the event horizon.

With the restriction on  $L/E$  for MHD accretion, we have discussed the secular evolution of black hole's rotation for certain magnetic flux-tubes. Although we have applied the boundary condition at the event horizon, our approach by the  $\xi$ -model guarantees that the ingoing MHD flow onto a black hole is trans-fast magnetosonic. Then, we find that there are two asymptotic states for the spin evolution. One is the state that (i) the angular velocity of the black hole approaches to that of the magnetic field line,  $\omega_H \rightarrow \Omega_F$ , and the other is the state that (ii) the spin-up due to angular momentum influx and the spin-down due to ingoing mass influx of MHD flows are canceled, where  $\tilde{L}\Omega_F = (\tilde{L}\Omega_F)_\omega$  is achieved. For type I case the asymptotic state of  $\delta\omega_H = 0$  is achieved when  $\tilde{L}\Omega_F = (\tilde{L}\Omega_F)_\omega$  (see Fig. 5a), although the state (i) of  $\omega_H \rightarrow \Omega_F$  may be realized before the state (ii). In the case of type II (see Fig. 5b), when  $L > 0$  the asymptotic state is given by  $\tilde{L}\Omega_F = (\tilde{L}\Omega_F)_\omega$ , while the spin terminates as  $\omega_H \rightarrow \Omega_F$  when  $L < 0$ .

When we discuss the actual asymptotic state in astrophysical situations, we should integrate the magnetic flux-tubes over the event horizon. Although we can speculate on the final stage that the angular velocity of the black hole will be settled to a typical value of that of the whole magnetic field lines connected to the event horizon, we need to construct a reasonable MHD accretion model under a certain magnetic field configuration to specify the functions  $L(\Psi)$  and  $E(\Psi)$ . The basic idea of the black hole-disk connection of magnetic field lines has been sug-

gested by some authors (e.g., [16, 17, 18, 19, 20, 21]). The realistic features of magnetic field lines have been presented by [12, 15, 22, 23, 24, 25]. In an astrophysical point of view, the magnetic connection between the black hole and the disk would play a very important role. The power input/output from the black hole depends on the ingoing MHD flow properties and the shape of the magnetic field lines. The released energy of the plasma in the deep gravitational potential well can be carried directly from the distant disk surface to the horizon by the black hole–disk connecting magnetic field lines. Furthermore, when the black hole is rapidly rotating, the rotational energy of the black hole can be carried from the black hole to the disk through magnetic interactions. Such energy and angular momentum transport from the disk to the black hole determines the fate of hole’s rotation.

Although in this paper a stationary magnetosphere is

discussed, their dynamical phase is also an important problem. The structure of a magnetosphere around the black hole is also discussed in [26, 27, 28, 29] by general relativistic MHD numerical simulations. Our current investigations performed by analytical methods can help gain deeper insight from the results obtained by time-dependent general relativistic MHD simulations.

### Acknowledgments

M.T. would like to thank Sachiko Tsuruta and Rohta Takahashi for their helpful comments. This work was supported in part by the Grants-in-Aid of the Ministry of Education, Culture, Sports, Science and Technology of Japan (17030006, 19540282, M.T.).

- 
- [1] S. A. Balbus, & J. F. Hawly, *Rev. Mod. Phys.*, 70, 1 (1998)
  - [2] D. L. Meier, *astro-ph/0504511* (2005)
  - [3] P. Ghosh, & F. K. Lamb, *ApJ*, 234, 296 (1979)
  - [4] J. M. Bardeen, *Nature*, 226, 64 (1970)
  - [5] K. S. Thorne, *ApJ*, 191, 507 (1974)
  - [6] R. D. Blandford, & R. L. Znajek, *MNRAS*, 179, 433 (1977)
  - [7] M. Takahashi, S. Nitta, Y. Tatematsu, & A. Tomimatsu, *ApJ*, 363, 206 (1990)
  - [8] S. J. Park, & E. T. Vishniac, *ApJ*, 332, 135 (1988)
  - [9] E. J. Weber, & L. Davis, Jr., *ApJ*, 148, 217 (1967)
  - [10] M. Camenzind, *A & A*, 162, 32 (1986)
  - [11] M. Takahashi, *ApJ*, 570, 264 (2002)
  - [12] S. Nitta, M. Takahashi, & A. Tomimatsu, *Phys. Rev.*, D44, 2295 (1991)
  - [13] A. Tomimatsu, & M. Takahashi, *ApJ*, 592, 321 (2003)
  - [14] J. M. Bardeen, W. H. Press, & S. A. Teukolsky, *ApJ*, 178, 347 (1973)
  - [15] A. Tomimatsu, & M. Takahashi, *ApJ*, 552, 710 (2001)
  - [16] K. Hirokuni, M. Takahashi, S. Nitta, & A. Tomimatsu, *ApJ*, 386, 455 (1992)
  - [17] C. F. Gammie, *ApJ*, 522, L57 (1999)
  - [18] P. Ghosh, & M. A. Abramowicz, *MNRAS*, 292, 887 (1997)
  - [19] L. -X. Li, *ApJ*, 567, 463 (2002)
  - [20] L. -X. Li, *PASJ*, 56, 685 (2002)
  - [21] M. H. P. M. van Putten and A. Levinson, *ApJ*, 584, 937 (2003)
  - [22] V. S. Beskin, *Physics-Uspeski*, 40, 659 (1997)
  - [23] P. Ghosh, *MNRAS*, 315, 89 (2000)
  - [24] D. A. Uzdensky, *ApJ*, 603, 652 (2004)
  - [25] D. A. Uzdensky, *ApJ*, 620, 889 (2005)
  - [26] S. Koide, D. L. Meier, K. Shibata, & T. Kudoh, *ApJ*, 536, 668 (2000)
  - [27] S. Hirose, J. H. Krolik, J. P. De Villiers, & J. H. Hawley, *ApJ*, 606, 1083 (2004)
  - [28] J. C. McKinney, & C. F. Gammie, *ApJ*, 611, 977 (2004)
  - [29] J. C. McKinney, *MNRAS*, 368, 1561 (2006)
  - [30] B. Punsly, *Black Hole Gravito-hydro-magnetics*, (Springer, Berlin, 2001)

### APPENDIX A: BENDING ANGLE OF MAGNETIC FIELD LINES

We will discuss the conditions on the electric-to-magnetic field amplitude function  $\xi$  or the bending angle  $\beta$  along a magnetic field line connected between the disk surface and the black hole. For a given function  $\xi^2 = \xi^2(r; \Psi)$  or  $\beta^2 = \beta^2(r; \Psi)$  we can easily obtain a trans-fast magnetosonic accretion solution  $M^2 = M^2(r; \Psi)$  by the quadratic equation as discussed in § III. To obtain a physically acceptable accretion solution, however, we should discuss some requirements on the function  $\xi$  at some characteristic radii, where some conditions may restrict the functional form of  $\xi^2$ . To discuss these requirements on  $\xi^2$ , we will consider a disk – black hole connecting magnetic field line, where the plasma injected from the disk surface streams toward the black hole along a magnetic field line. First, the magnetic field line would almost corotate with the “footpoint” on the plasma source, where the magnetic field line is anchored. So we may expect  $B_\phi \sim 0$  ( $\beta^2 \gg 1$ ) there when the toroidal surface current dominates the poloidal one, or  $\beta^2 \sim O(1)$  when the toroidal surface current is almost the same as the poloidal one.

In the cases of type I and III, the ingoing plasma injected from the disk surface may bend the magnetic field toward the counterrotating direction (the trailed-shape of the magnetic field line:  $B_\phi < 0$ ) due to the plasma inertia effect. This situation is analogous to pulsar magnetosphere, although the magnetic field lines extend inwardly to the black hole. Conversely, the plasma flow ejected toward the rotation direction (the leading-shaped:  $B_\phi > 0$ ) may be also possible. In this case, however, the magnetic field line flips over at the “anchor point” (see also [30]), which corresponds to the Alfvén radius of  $M^2 \neq \alpha$  (where  $B_\phi = 0$ ). At the anchor point, we see that  $\xi^2 = \infty$  and  $\beta^2 = 0$ . At the Alfvén point that is the Alfvén radius

TABLE I: Restrictions on the functions  $\xi^2$  and  $\beta^2$  at various characteristic radii are summarized. The radius appeared in accretion solution is marked by “o” for types I/III and II, while the mark “x” shows the absence of that radius in the solution.

Characteristic Radii	$\xi^2$	$\beta^2$	I/III	II
Event Horizon (H) $r_H$	1	$-\alpha_H$	o	o
Corotation point (C) $r_\omega$	0	finite	x	o
Alfvén Point (A) $r_A$	finite	finite	o	o
Anchor point (AN) $r_{AN}$	$\infty$	0	o	x
Plasma source (I) $r_I$	finite	finite	o	o

with the condition  $M^2 = \alpha$ , we see  $B_\phi \neq 0$  and both  $\xi^2$  and  $\beta^2$  have finite values.

Next, in type II case, the rotating black hole must bend the magnetic field toward the rotating direction ( $B_\phi > 0$ ). In this type, no anchor point exists, but the “corotation point” where  $\Omega_F = \omega$  exists between the inner and outer light surface, while in type I and III cases no corotation point exists on the way to the event horizon. The value of  $\xi$  at the corotation point, where  $Y = 0$ , must become zero (i.e.,  $1 + X = 0$ ) to avoid the  $A < 0$  region near the corotation point, while  $\beta^2$  has a finite value there. [If not so, we obtain  $(\tilde{L}\Omega_F)^+ = (\tilde{L}\Omega_F)^- = 0$  at the corotation point, and we see the  $A < 0$  region between the plasma source and the event horizon; that is, no physical ingoing solution exists.] Finally, at the event horizon, the boundary condition there requires that  $\xi_H^2 = 1$  or  $\beta_H^2 = -\alpha_H$ . These requirements on  $\xi$  at characteristic radii are summarized in Table I.

For example, for type I and III cases, we can simply set a model with  $\xi^2(r, \theta) = \xi_H^2 = 1$  throughout the flow region considered for ingoing flows without the anchor point. (Here, we consider a situation that the plasma source is placed inside the anchor point.) As another example, we may add a deviation term from the  $\xi^2(r, \theta) = 1$  model, which must become zero on the event horizon, as follows;

$$\xi^2 = 1 + C_I \left( \frac{\Delta}{\Sigma} \right), \quad (\text{A1})$$

where  $C_I$  is a constant.

To see the behaviors of accretion onto the black hole in type II case, however, we should consider the function  $\xi$  to satisfy both the boundary condition at the event horizon and the requirement on the corotation point. Then, for example, we will consider the following function for  $\xi$ ,

$$\xi^2 = \left[ 1 + C_{II} \left( \frac{\Delta}{\Sigma} \right) \right] \left( \frac{\omega - \Omega_F}{\omega_H - \Omega_F} \right)^2, \quad (\text{A2})$$

where  $C_{II}$  is a constant. [The functions  $(\tilde{L}\Omega_F)^\pm$  seen in Figure 3d could be plotted under this distribution of  $\xi$ .] Note that the  $\xi^2(r, \theta) = 1$  inflow model in the type II case requires  $\beta = 0$  at the corotation point. This requirement

means  $B_\phi = 0$  that corresponds to the anchor point, but there is *no* anchor point in type II flow solutions. Thus, the simple  $\xi^2(r, \theta) = 1$  model can not be applied as an inflow solution for a rapidly rotating black hole (type II) case.

For outflows ( $r \gg m$ ), for example, we can make a model

$$\xi^2 = 1 - \frac{1}{\hat{E}^2} + \zeta_0, \quad (\text{A3})$$

where  $\zeta_0$  is the parameter for the magnetic field geometry. For  $\zeta_0 < 0$ , the outgoing flow reaches the distant region with a finite Mach number, while for  $\zeta_0 > 0$  the flow is confined within a certain radius  $R_c$  where the Mach number becomes to diverge (see [13], for detail discussions).

In a realistic situation for the black hole magnetosphere, a global structure of magnetic field lines would not be able to be expressed by simple forms of function  $\xi$ . To understand the basic properties of MHD inflows/outflows, it will be helpful to use function (A1) or (A2) for ingoing winds and function (A3) for outgoing winds. In § III, we show Figures 1 and 2 that are accretion solutions *along a given stream line* with a given function  $\xi(r; \Psi)$ . However, we should note that, as a practical matter, we can obtain *the velocity distribution*  $u^r(r, \theta)$  in the poloidal plane when the function  $\xi(r, \theta)$  is specified as a model.

Now, we consider the restriction on the function  $\xi(r, \theta)$  for the  $A > 0$  region, which is the necessary condition for MHD ingoing/outgoing winds, in the black hole magnetosphere. If the discriminant in equation (26) becomes zero at some location  $(r, \theta)$  in the super-Alfvénic region, equation (26) becomes

$$(\tilde{L}\Omega_F)^+ = (\tilde{L}\Omega_F)^- = (\tilde{L}\Omega_F)_d, \quad (\text{A4})$$

where

$$(\tilde{L}\Omega_F)_d \equiv 1 - \frac{G_t}{\hat{E}^2}, \quad (\text{A5})$$

and the corresponding  $\xi_d^2$  value,  $\xi_d^2$ , is expressed as

$$\xi_d^2(r, \theta) \equiv \frac{g_{\phi\phi}(\Omega_F - \omega)^2 (g_{tt} - \hat{E}^2)}{G_t^2 - \alpha \hat{E}^2}. \quad (\text{A6})$$

Under the condition of  $\xi^2(r; \Psi) < \xi_d^2(r; \Psi)$  along a magnetic field line  $\Psi = \Psi(r, \theta)$ , the requirement  $A > 0$  on the super-Alfvénic solution is possible for a suitable  $\tilde{L}\Omega_F$  value at most in the magnetosphere. If the situation with  $\xi^2(r; \Psi) = \xi_d^2$  is achieved on the magnetic field line considered, the  $A = 0$  surface must appear on the way to the  $\xi^2 = \xi_d^2$  radius (i.e., between the plasma source and the location with  $\xi^2 = \xi_d^2$ ). Such a situation gives an unphysical flow solution. Note that, for the inflow, if the  $\xi^2 = \xi_d^2$  surface encloses the event horizon, no black hole accretion solution exists. Although the value of  $\xi_d^2$  diverges ( $\xi_d^2 = \pm\infty$ ) at surfaces with  $\alpha/G_t^2 = 1/\hat{E}^2$  [ or  $Y = (\tilde{L}\Omega_F)_d$  ], the inner and outer

surfaces of  $\xi_d^2(r, \theta) = \infty$  exist in the black hole magnetosphere. Between these surfaces, the value of  $\xi_d^2$  is always negative and the discriminant in equation (26) is positive; that is, the condition  $A > 0$  is achieved everywhere. This  $\xi_d^2 < 0$  region occupies the magnetosphere at most between the inner and outer light surfaces. For the  $\hat{E} \gg 1$  flow, the  $\xi_d^2(r, \theta) = \infty$  surfaces coincide with the light surfaces (given by  $\alpha = G_t^2/\hat{E}^2 \sim 0$ ). Thus, for accretion/wind solutions, the condition  $\xi^2(r; \Psi) < \xi_d^2(r; \Psi)$  must be required along a magnetic field line considered, except for the  $\xi_d^2 < 0$  region.

## APPENDIX B: THE RESTRICTION ON THE ALFVÉN POINT BY THE $A > 0$ CONDITION

Here, we consider the restriction on the Alfvén point due to the condition  $A > 0$  for the MHD accretion solution again (see § IV A). Although the relation  $\tilde{L}\Omega_F = Y_A$  gives the Alfvén surface, the Alfvén surface must be located within the  $A > 0$  region. Then, the innermost limit of the inner Alfvén point (marked by  $A_*$ ) for a given magnetic flux surface is given by  $Y_{A_*} = (\tilde{L}\Omega_F)_{A_*}^+$  for type I and III, and  $Y_{A_*} = (\tilde{L}\Omega_F)_{A_*}^-$  for type II, whose relation can be reduced to

$$(\tilde{L}\Omega_F)_{A_*} \equiv Y_{A_*} = 1 - \frac{(G_t)_{A_*}}{\hat{E}^2}. \quad (\text{B1})$$

Note that this relation is independent of the function  $\xi$ . If the Alfvén point is located inside this critical location, the location with  $A = 0$  appears in the super-Alfvénic region. Then, the requirement for the acceptable  $\tilde{L}\Omega_F$  range discussed in § IV A should be modified to avoid such a situation (see, Figs 3c and 3d, where the location of  $r = r_{A_*}$  is given by the fill circle on the  $\tilde{L}\Omega_F = Y$  curve). That is, we should take the range with  $(\tilde{L}\Omega_F)_{A_*} < \tilde{L}\Omega_F$  for the  $E < 0$  inflows in the type II case, where  $(\tilde{L}\Omega_F)_{A_*} > 1$ . On the other hand, we should take the range with  $\tilde{L}\Omega_F < (\tilde{L}\Omega_F)_{A_*}$  for the inflows ( $E > 0$ ) in the type I and III cases, where  $(\tilde{L}\Omega_F)_{A_*} < 1$ .

Thus, with respect to  $\tilde{L}\Omega_F$  for the black hole accreting flows, we summarize the necessary condition with

$$|1 - \tilde{L}\Omega_F| > \frac{|(G_t)_{A_*}|}{\hat{E}^2}. \quad (\text{B2})$$

If not so,  $A = 0$  is realized between the inner Alfvén point and the event horizon; that is, the Mach number of the trans-Alfvénic solution diverges there (unphysical). When we consider the trans-Alfvénic ingoing flow, for  $r_A > r_{A_*}$  equation (B2) can be rewritten as  $\hat{e}^2 > \alpha_A$ , which gives a physical solution. However, no physical trans-Alfvénic flow, where  $u_p^2(r_A) < 0$ , is obtained for  $r_A \leq r_{A_*}$ .

When we treat a magnetically-dominated flow with  $\hat{E} \gg 1$ , we should mention the deviation from the limit of large magnetization; i.e., the force-free case. (In the

magnetically-dominated flow limit, we see that  $\hat{E} \rightarrow \infty$ ,  $\tilde{L}\Omega_F \rightarrow 1$  and  $r_{A_*} \rightarrow r_L^{\text{in}}$ .) For the magnetically-dominated flow, the deviation from the force-free model with respect to the  $\tilde{L}\Omega_F$  value is of the order of  $\hat{E}^{-2}$ , and the location of the Alfvén point also separates from the inner light surface in the same order [ $(r_{A_*}/r_L) = 1 + |O(\hat{E}^{-2})|$ ]. When we discuss some problems (e.g., the energy and angular momentum transport) in the MHD framework, the deviation from the force-free model becomes important. This necessary condition for the trans-Alfvénic flow solutions discussed above also applies to the outflows.

## APPENDIX C: THE NATURE OF THE PARAMETER $\chi$

In V A, we introduced the function  $\chi$  that represents the magnetic field configuration near the event horizon. Although the function  $\chi(\theta_H)$  should be given by solving the GS equation, in this paper we only treat it as a parameter without the GS equation. Here, we discuss the characteristic nature of the parameter  $\chi$ .

First, we consider the maximum  $\chi$  value ( $\equiv \chi_{\text{max}}$ ) for existing  $A > 0$  region in both type I and II cases, where we obtain

$$\chi_{\text{max}} \equiv \frac{1 + [(\Omega_F^2 - \omega_H^2)/\omega_H^2](g_{tt}^H/\hat{E}^2)}{\mathcal{H}[(\Omega_F - \omega_H)/\omega_H](1 - g_{tt}^H/\hat{E}^2)}, \quad (\text{C1})$$

which gives  $(\tilde{L}\Omega_F)_H^+ = (\tilde{L}\Omega_F)_H^-$ . In the Schwarzschild black hole case, we have  $\chi_{\text{max}} \sim (2m\Omega_F \sin\theta)^{-2}$ , which is finite near the equator. When  $\chi > \chi_{\text{max}}$ , no physical trans-fast magnetosonic accretion solution exists for any  $\tilde{L}\Omega_F$  values. On the other hand, we have that  $(\tilde{L}\Omega_F)_H^+ \sim (\tilde{L}\Omega_F)_H^- \sim \Omega_F/\omega_H = Y_H$  when  $(-\chi) \gg 1$ .

Second, we see that the value of  $(\tilde{L}\Omega_F)_H^\pm$  diverges when

$$\chi = \chi_\infty \equiv -(\omega_H + \Omega_F)/(\mathcal{H}\omega_H), \quad (\text{C2})$$

while  $(\tilde{L}\Omega_F)_H^-$  is finite. For a rapidly rotating black hole case (type II) this situation,  $\chi = \chi_\infty$ , arises in the  $\chi > 0$  region (see Fig. 4b). For a slowly rotating black hole case (type I), however, the value of  $\chi_\infty$  is always negative, and then no restriction by the  $A_H < 0$  condition exists on the acceptable  $\tilde{L}\Omega_F$  range (see Fig. 4a). Furthermore, we also specify the third value

$$\chi_0 \equiv -[(r_H - m)\Sigma_H/(2m^2r_H)]/\hat{E}^2, \quad (\text{C3})$$

where the function  $(\tilde{L}\Omega_F)_H^\pm$  becomes zero. Although the function  $(\tilde{L}\Omega_F)_H^\pm$  has a  $\hat{E}$  dependence, the dependence is weak for  $\hat{E} > 1$ . In the limit of  $\hat{E} = \infty$ , we see that  $\chi_0 = 0$ , where  $(\tilde{L}\Omega_F)_H^+ = 0$ , and  $\chi_{\text{max}} = \chi_\infty \omega_H^2/(\Omega_F^2 - \omega_H^2)$ , where  $(\tilde{L}\Omega_F)_H^\pm = 1$ , while  $\chi_\infty$  is independent of  $\hat{E}$ .

In §IV B we introduce the restrictions on  $\tilde{L}\Omega_F$  by the condition (B2) at the Alfvén point. The additional restriction from the boundary condition at the event horizon should be also imposed to avoid the  $A = 0$  surface

on the super-Alfvénic accretion flow. Then, the ingoing flow solution can be classified by the  $\chi$  value. First, for the slowly rotating black hole case (type I), the ranges of  $\tilde{L}\Omega_F < (\tilde{L}\Omega_F)_H^-$  and  $\tilde{L}\Omega_F > (\tilde{L}\Omega_F)_H^+$  are forbidden from the boundary condition at the event horizon. In addition to this restriction, the range of  $\tilde{L}\Omega_F < (\tilde{L}\Omega_F)_{\min}$  and  $(\tilde{L}\Omega_F)_{A^*} < \tilde{L}\Omega_F$  are also forbidden from the condition of the Alfvén point, where  $(\tilde{L}\Omega_F)_{A^*} < 1$  for type I case. When  $\chi < \chi_{\max}$ , the acceptable range of  $\tilde{L}\Omega_F$  is given by  $\text{MAX}[(\tilde{L}\Omega_F)_{\min}, (\tilde{L}\Omega_F)_H^-] < \tilde{L}\Omega_F < (\tilde{L}\Omega_F)_{A^*}$  for the magneto-like accretion solution, while that is  $\text{MAX}[(\tilde{L}\Omega_F)_{\min}, (\tilde{L}\Omega_F)_H^-] < \tilde{L}\Omega_F < (\tilde{L}\Omega_F)_{\min}^+ < (\tilde{L}\Omega_F)_{A^*}$  for the hydro-like accretion solution, where  $(\tilde{L}\Omega_F)_{\min}^+$  is the minimum of the function  $(\tilde{L}\Omega_F)^+ = (\tilde{L}\Omega_F)^+(r)$  (see also Fig. 3c). Note that  $(\tilde{L}\Omega_F)_H^- < 0$  for  $\chi < \chi_0$ , while the value of  $(\tilde{L}\Omega_F)^{\min}$  is always positive. For type III case, we can see the similar behavior of  $\tilde{L}\Omega_F$ .

Next, for a rapidly rotating black hole case (type II), the value of  $\chi$  is related to the signature of the total energy  $E$  and angular momentum  $L$  of the flow. When  $\chi < \chi_\infty$  the accretion solution in the range  $(\tilde{L}\Omega_F)_H^+ < \tilde{L}\Omega_F < (\tilde{L}\Omega_F)_H^-$  must be forbidden from the boundary condition at the event horizon, and when  $\chi_\infty < \chi < \chi_{\max}$  the solution in the ranges  $\tilde{L}\Omega_F < (\tilde{L}\Omega_F)_H^-$  and  $\tilde{L}\Omega_F > (\tilde{L}\Omega_F)_H^+$  must be forbidden. Furthermore, the range  $(\tilde{L}\Omega_F)_H^- < \tilde{L}\Omega_F < (\tilde{L}\Omega_F)_{A^*}$ , where  $(\tilde{L}\Omega_F)_{A^*} > 1$  for accretion solutions in type II, is also forbidden by the existence of the  $A = 0$  surface between the Alfvén point and the event horizon as mentioned in §IV B. Then, we obtain the acceptable ranges as  $\tilde{L}\Omega_F < (\tilde{L}\Omega_F)_H^+$  and  $\tilde{L}\Omega_F > (\tilde{L}\Omega_F)_{A^*}$  for ingoing flows with  $\chi < \chi_\infty$ , while the acceptable range is  $(\tilde{L}\Omega_F)_{A^*} < \tilde{L}\Omega_F < (\tilde{L}\Omega_F)_H^+$  for inflows with  $\chi_\infty < \chi < \chi_{\max}$ .

Here, we will consider three ranges of  $\chi$ -value for type

II case; that is,

(a)  $\chi_\infty < \chi < \chi_{\max}$ ,

(b)  $\chi_0 < \chi < \chi_\infty$ ,

(c)  $\chi < \chi_0$ .

In all cases, the negative energy inflow is acceptable. In the cases (b) and (c) the positive energy inflow is also possible, while in the case (a) energy  $E$  must be negative. Thus, the value  $\chi_\infty$  gives the maximum  $\chi$  value for the positive energy input to the black hole. Similarly, for the cases (a) and (b), the angular momentum of the inflows must be negative, while in the case (c) both the positive and negative inflows are available. The  $\chi = 0$  inflow is included in the case (b); the example of  $(\tilde{L}\Omega_F) = (\tilde{L}\Omega_F)^\pm(r)$  curve shown in Figure 3b corresponds to this case. When we consider the  $a \rightarrow m$  limit, where  $\mathcal{H} \rightarrow \infty$ , we obtain  $(\tilde{L}\Omega_F)_H^\pm(\chi) \rightarrow Y_H = 2m\Omega_F$ , and  $\chi_{\max} \rightarrow 0$ ,  $\chi_\infty \rightarrow 0$  and  $\chi_0 \rightarrow 0$ . Then, only  $\chi < 0$  is acceptable, which gives the acceptable  $\tilde{L}\Omega_F$  of  $\tilde{L}\Omega_F < Y_H$  and  $(\tilde{L}\Omega_F)_{A^*} < \tilde{L}\Omega_F$ . When  $\omega_H \rightarrow \Omega_F$ , we have  $\mathcal{H} = 0$ ,  $\chi_{\max} \rightarrow \infty$ ,  $\chi_\infty \rightarrow \infty$ ,  $(\tilde{L}\Omega_F)_H^-(\chi) = 1$  and  $(\tilde{L}\Omega_F)_H^+(\chi) = 0$ . The acceptable  $\tilde{L}\Omega_F$  ranges are  $\tilde{L}\Omega_F < 0$  and  $(\tilde{L}\Omega_F)_{A^*} < \tilde{L}\Omega_F$ ; only negative angular momentum flows are available. For the off-equatorial inflow of  $\theta \ll 1$ , we have  $\mathcal{H} \propto \sin^2 \theta$ ,  $|\chi_\infty| \propto \sin^{-2} \theta$  and  $\chi_{\max} \propto \sin^{-2} \theta$ , while the value of  $\chi_\infty$  does not change drastically. Just on the pole, we find that  $(\tilde{L}\Omega_F)_H^+ \sim 0$  and that for the type II case only the inflow with  $L \leq 0$  is available. Thus, the ratio of the toroidal and poloidal magnetic fields that is related to the bending angle of the magnetic field line is restricted by the total energy and angular momentum of accretion onto a rotating black hole.